JOURNAL OF GEOPHYSICAL RESEARCH, VOL. 105, NO. A8, PAGES 18,251–18,274, AUGUST 1, 2000

Energetic proton observations at 1 and 5 AU 2. Rising phase of the solar cycle 23

D. Lario,[1,2] R. G. Marsden,[1] T. R. Sanderson,[1] M. Maksimovic,[1,3] B. Sanahuja,[4,5] S. P. Plunkett,[6] A. Balogh,[7] R. J. Forsyth,[7] R. P. Lin,[8] and J. T. Gosling[9]

Abstract. The increasing level of solar activity at the end of 1997 coincides with the observation of solar energetic particle (SEP) events by the Wind and Ulysses spacecraft. The proximity of Ulysses to the ecliptic plane during this period allows us to study the effects of the solar activity at two different heliolongitudinal and heliocentric distances but at similar heliolatitudes. We identify the main transient proton enhancements seen by Wind and Ulysses from October 1997 to the end of December 1998. We compare their characteristics and suggest an interpretation in terms of their heliospheric location, the activity occurring at the Sun, and the conditions for particle propagation between the Sun and both spacecraft. Whereas at 1 AU different SEP events can be associated with individual coronal mass ejections (CMEs), at 5 AU long-lasting SEP events are observed while a sequence of CMEs takes place at the Sun. Continuous injection of particles from traveling CME-driven shocks, the effects of particle propagation along interplanetary magnetic field lines, and the corotation of these field lines across the Ulysses location are the main factors responsible for these long-lasting periods of high particle intensity observed by Ulysses.

1. Introduction

Lario et al. [this issue, hereinafter referred to as paper 1] split the Ulysses proton observations during 1997–1998 in two periods: period 1 from January 1, 1997, to September 30, 1997; and period 2 from October 1, 1997, to December 31, 1998. Their division is based on the energy range of the particle flux enhancements observed by Ulysses, the time delay between the flux profiles at 1 and at ~5 AU, and the solar wind and magnetic field conditions scanned by Ulysses. Period 1 is characterized by a lack of high-energy (>8 MeV) proton events, long time delays (~10 days), and the presence of corotating high-speed solar wind streams arriving at Ulysses. Period 2 is characterized by a higher proton intensity, shorter time delays (~5 days), and a full immersion of Ulysses in the slow solar wind. Paper 1 concentrates on the analysis of period 1, while here we focus on the proton observations throughout period 2.

In this period, Ulysses moved from +3.7° to −19.0° in heliographic latitude. In October 1997, Ulysses was at 5.29 AU from the Sun and moving equatorward. In April 1998 it completed its first out-of-ecliptic orbit, reaching aphelion at 5.41 AU. By the end of 1998 it was at a heliocentric distance of 5.20 AU continuing its journey to southern latitudes. Throughout this period, several solar energetic particle (SEP) events were observed by Ulysses and by the other spacecraft located around the orbit of the Earth [*Lario et al*., 1998a; *Marsden et al*., 1999; *von Rosenvinge et al*., 1999]. The proximity of Ulysses to the ecliptic plane allows us to compare the effects of the solar activity on the particle populations at two different heliocentric distances (1 and ~5 AU) but at similar heliolatitudes.

The effects of solar activity on the particle populations are most prominent in the processes of particle acceleration occurring at the Sun and in the heliosphere. The most intense SEP events are produced by acceleration of particles at collisionless shock waves driven by coronal mass ejections (CMEs) [*Reames*, 1999]. Shock-accelerated particles are injected into the heliosphere and propagate along interplanetary magnetic field (IMF) lines. Particle flux enhancements are then observed if, at some time during the development of an SEP event, magnetic connection between the observer and the field lines along which these particles propagate is established. Whereas CME-driven shocks may accelerate protons to energies as high as 1 GeV [*Kahler*, 1994], they are not thought to be efficient accelerators of electrons [*Lee*, 1997]. Proton flux increases at energies below 20 MeV are frequently observed at 1 AU from a large range of longitudes regardless of the solar longitude where the CME originated [*Cane et al*., 1988]. Relativistic electrons, however, are only occasionally observed from large angular distances with respect to the parent solar event [*Kallenrode et al*., 1992]. Energetic particle events with high electron-to-proton ratios are usually observed by spacecraft magnetically well connected to the site where the solar event occurred [*Cane et al*., 1986]. The prompt arrival of relativistic electrons at the spacecraft after the occurrence of a solar event and the observation of an SEP event with a strong electron component suggest a good magnetic connection between the

[1]Space Science Department of European Space Agency, ESTEC, Noordwijk, Netherlands.
[2]Now at Applied Physics Laboratory, Johns Hopkins University, Laurel, Maryland.
[3]Now at DESPA, Observatoire de Meudon, Meudon, France.
[4]Departament d'Astronomia i Meteorologia, Universitat de Barcelona, Barcelona, Spain.
[5]Also at Institut d'Estudis Espacials de Catalunya, Barcelona, Spain.
[6]Universities Space Research Association, Naval Research Laboratory, Washington, D. C.
[7]Imperial College of Science and Technology, London, England.
[8]Space Sciences Laboratory, University of California, Berkeley.
[9]Los Alamos National Laboratory, Los Alamos, New Mexico.

Paper number 1999JA000374.
0148-0227/00/1999JA000374$09.00

observer and the region where the solar event occurred. The observation of particle events with low electron-to-proton ratios indicates that traveling shocks, at some time during their propagation, were able to inject energetic protons on to those magnetic field lines to which the observer establishes magnetic connection.

Analyses of SEP events have usually been restricted to 1 AU and inner heliospheric distances [*Cane et al*., 1988; *Heras et al*., 1992, 1995; *Kallenrode et al*., 1993; *Reames et al*., 1996]. At these distances the proton flux profiles take different forms depending on the heliolongitude of the source region, the evolution of the associated shocks (speeds, sizes and shapes), their efficiency in accelerating particles; the presence of a seed particle population capable of being accelerated, the conditions for the propagation of shock-accelerated particles, and the energy considered [e.g., *Lario et al*., 1998b, and references therein]. Figure 15 of *Cane et al*. [1988] gives a general overview of the proton flux profiles at ~20 MeV detected at 1 AU in terms of the observing longitudes relative to the location of the source of the CME generating an SEP event. The ~20 MeV proton flux profiles range from (1) a prompt increase shortly after the CME with a later gradual decay (for well-connected events, which for an observer near the Earth are SEP events generated from the west limb of the Sun, and thus called West-type events), to (2) a sudden increase shortly (a few hours) before the arrival of the interplanetary shock at the observer (for poorly connected events, which for an observer near the Earth are SEP events generated from the east limb of the Sun, and thus called East-type events), passing through (3) a gradual and progressing enhancement of the particle intensity from the moment of the CME up to the arrival of the CME-driven shock at the observer (for events occurring near the Central Meridian as seen by an observer near the Earth, and thus called Central Meridian–type events). Simulations of these type of events have been done by *Heras et al*. [1995] and *Lario et al*. [1998b] using the concept of the cobpoint which describes the magnetic connection between the observer and the shock front as the shock propagates away from the Sun.

Ulysses particle observations are more complicated to interpret. CME-driven interplanetary shocks take a long time to arrive at Ulysses (~11 days assuming a constant traveling speed of 800 km s^{-1} from the Sun to 5 AU). During periods of intense solar activity it is quite usual to observe several CMEs in the time that a shock takes to travel from the Sun to Ulysses. Furthermore, as interplanetary shocks expand in heliolongitude, they may cross and recross many IMF lines (assuming a Parker spiral structure). The occurrence of multiple CMEs and the difficulty of delimiting the Ulysses magnetic field connection with traveling shocks complicate the identification of the source of the particles. In addition, the effects due to particle transport through the heliosphere and the effects due to the motion of the magnetic field lines frozen in the solar wind (known as the corotation effect (paper 1)) modulate the final shape of the proton flux profiles in such a way that they may blur any signature of the source where these particles were accelerated.

As a consequence of all these processes, we expect that SEP events in the outer heliosphere will show different characteristics than at 1 AU. Particularly, we expect longer time durations for the SEP events due to (1) the more numerous interplanetary processes acting on the particles throughout their longer journey; (2) the new particle injections coming from new solar events (and their related shocks) sustaining a high proton flux for a longer time; and (3) the modulation of the flux profiles caused by the arrival of different traveling structures able to channel, trap and accelerate energetic particles (corotating flux tubes, interplanetary shocks, magnetic clouds, etc.). We also expect a different contribution from a given CME-driven shock to the observed flux profile, depending on which parts of the shock front establish magnetic connection with the spacecraft and on which phase of its journey from the Sun to Ulysses the shock gets connected or disconnected from the observer.

With the aim of analyzing these processes we compare the observations of SEP events at 1 and ~5 AU during the rising phase of the solar cycle 23. In this paper we cover the whole period 2, which constitutes a unique opportunity to contrast the effects of solar activity on the particle population in the inner (~1 AU) and outer (~5 AU) heliosphere. Ulysses' location and the observation of several discrete episodes of intense solar activity at the end of 1997 and throughout 1998 make this period suitable for analysis. First, we identify the solar events responsible for the origin of the SEP events at 1 AU, and then we suggest possible scenarios under which these SEP events developed in the outer heliosphere. In section 2 we present the data sources and the criteria to select the specific SEP events to analyze. In section 3 we describe the data for these SEP events at 1 and 5 AU and discuss the suggested scenarios. In section 4 we summarize the main factors that account for the different flux profiles of the SEP events observed in the inner and outer heliosphere, and we discuss the CME parameters that determine the production of SEP events at 1 AU. Finally, in section 5 we present the main conclusions of this work.

2. Instrumentation, Observations, and Selection of Events

Ulysses particle observations presented in this paper were made with the Low Energy Telescope (LET) of the Cosmic Ray and Solar Particle Investigation (COSPIN) instrumentation [*Simpson et al*., 1992]. We use the 10-min-averaged proton flux in the range from 1.2 to 19 MeV. We also use high-energy (2.5–7.0 MeV) electron observations from the Kiel Electron Telescope (KET) of the COSPIN instrument [*Simpson et al*., 1992] in order to determine the contribution of traveling interplanetary shocks to the observed SEP event. Data from the solar wind plasma experiment [*Bame et al*., 1992] and the magnetometer [*Balogh et al*., 1992] have also been used in the interpretation of the SEP events at Ulysses.

Observations close to 1 AU were made by the 3*DP* instrument aboard Wind [*Lin et al*., 1995]. This spacecraft executed complex orbits between the Earth and the Sun-Earth Lagrangian point L1, spending most of the time in the solar wind outside the Earth's magnetosphere. In November 1998, Wind was placed in a new petal orbit around the Earth with a ~10 R_E perigee and ~80 R_E apogee, which allowed consecutive encounters by this spacecraft with the Earth's magnetosphere. We use observations of energetic protons from the 3*DP* instrument in the energy range from 400 keV to 13.5 MeV. Although the 3*DP* instrumentation did not resolve protons from alphas and heavier ions, their contribution (small compared to the more numerous protons) does not affect the description of the particle events included in this paper. We also use observations from the Wind magnetometer MFI instrument [*Lepping et al*., 1995] to identify magnetic field struc-

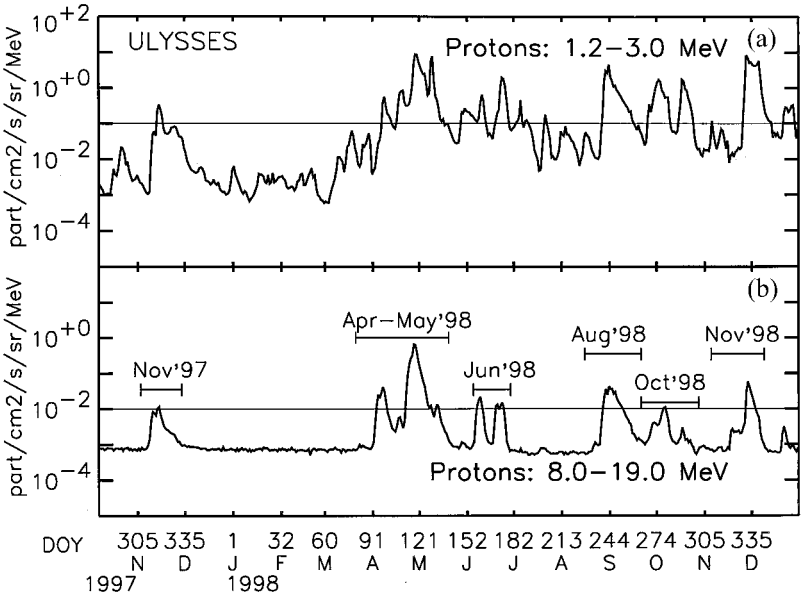

Figure 1. One-day averages of (a) 1.2–3.0 MeV and (b) 8.0–19.0 MeV proton fluxes as measured with the Ulysses/COSPIN/LET experiment from October 1997 to December 1998. Horizontal lines mark the criterion to select the time intervals to analyze.

tures arriving at Wind. Interplanetary shocks and magnetic clouds have been identified by the Wind/MFI team (list accessible on http://lepmfi.gsfc.nasa.gov/).

In order to relate the observation of SEP events at both spacecraft to solar events occurring at the Sun, we use published analyses of the same events and/or the observation of CMEs by the Large Angle Spectrometric Coronagraph (LASCO) on the SOHO spacecraft [*Brueckner et al*., 1995]. Lists of CMEs observed by LASCO are available on ftp://lasco6.nascom.nasa.gov/pub/lasco/status/. The source longitude of CMEs cannot be directly determined from coronagraph observations. Fortunately, the large solar events considered in this work are usually accompanied by either solar flares or filament disappearances (FD). We use the list of solar flares and FDs of Boulder Preliminary Reports (BPR) (http://www.sec.noaa.gov/weekly.html, 1997, 1998) and Solar Geophysical Data (SGD) as indicative of the angular direction of the expanding CMEs, keeping in mind that flares are not necessarily centered on the CMEs and angular errors might exist [*Harrison*, 1995]. When LASCO images are not available, we use the list of CMEs observed with the Mark III K coronameter at Mauna Loa Solar Observatory (MLSO) [*Fisher et al*., 1981]. Note that MLSO observing day begins ~1700 UT and can end as late as 0330 UT the next day. The details of CME identification and measurement by MLSO are available on http://www.hao.ucar.edu/public/research/. From CME images it is possible to obtain information about the direction of propagation of the CMEs as well as their angular width ω. The location of the CME leading edge in successive coronagraph pictures allows us to estimate its propagation speed v_{CME}. This speed is a projection in the plane of the sky where pictures have been taken. When a CME occurs close to the limb of the Sun, v_{CME} is related to its actual propagation speed in the interplanetary medium; however, when it propagates in other directions, v_{CME} is subject to projection effects. In the same way, owing to the three-dimensional structure of the CMEs, single coronagraph observations do not allow us to infer their longitudinal spreads. The apparent angular widths of the CMEs, ω, are only included in this study as indicative of their sizes seen from coronagraph observations, but they cannot be directly related to the extent in the ecliptic plane of the shocks driven by them. The times given for the CMEs throughout this paper refer to their first appearance in the LASCO C2 (>2 R_s) or MLSO MK3 coronagraph (>1.12 R_s).

Figure 1 shows 1-day averages of the 1.2–3.0 MeV (Figure 1a top) and 8.0–19.0 MeV (Figure 1b) proton fluxes observed by Ulysses from October 1997 to the end of December 1998. We have selected several periods based on their proton intensity, in particular those periods with a 1.2–3.0 MeV proton flux above 10^{-1} proton/(cm^2 s sr MeV) and 8.0–19.0 MeV proton flux above 10^{-2} proton/(cm^2 s sr MeV). We have designated each one of these periods by the name of the month when the main particle enhancement occurs (see the corresponding interval in Figure 1b). We have shown in paper 1 that there is a temporal association between particle flux enhancements observed by Wind and Ulysses. The duration of each one of these intervals is such that it includes the complete period of the proton flux enhancement at 1 AU (see Figure 1 in paper 1).

Figure 2 shows the 2.5–7.0 MeV electron intensity observed by Ulysses from October 1997 to the end of December 1998. These highly relativistic electrons are thought to propagate directly from their source region to the observer without experiencing significant deflection due to scattering processes. We have indicated in Figure 2 the periods selected for study on the basis of their high proton intensity (Figure 1). As can be seen, there is little correlation between the electron events and the proton flux enhancements. The period of August 1998, for example, is characterized by a high proton intensity, but it does not show any significant electron enhancement at these energies. The values for the electron intensity outside the periods of November 1997, April–May 1998, and November 1998 (i.e., those intervals without a high electron intensity) have to be taken with caution because of instrumental background due to secondary electrons (B. Heber, private communication, 1999).

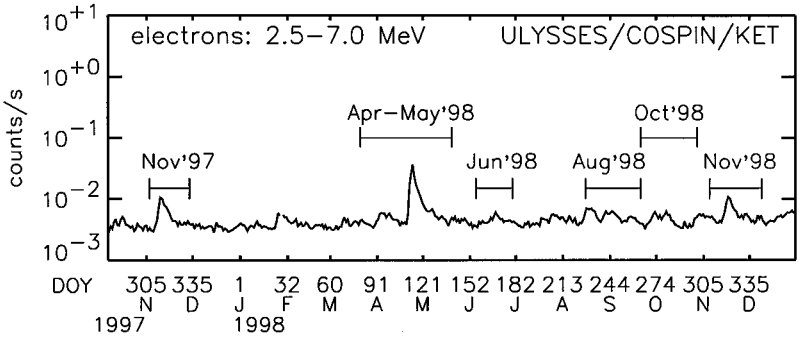

Figure 2. One-day averages of 2.5–7.0 MeV electron intensity as measured by the Ulysses/COSPIN/KET experiment from October 1997 to December 1998.

3. Scenario for the Particle Events

Figures 3–8 show the periods selected for detailed analysis. In the top panel we present Wind observations: 10-min averages of the 400 keV to 10.7 MeV proton flux, the solar wind speed (V), the magnetic field magnitude ($|\mathbf{B}|$), and its direction (θ is the polar angle and ϕ the azimuth angle in a GSE coordinate system). In the middle panel we present Ulysses observations: 1-hour averages of the 1.2–19 MeV proton flux, the solar wind speed as measured by the Ulysses solar wind plasma experiment, the magnetic field magnitude ($|\mathbf{B}|$) and its direction in the Ulysses RTN coordinate system. Interplanetary shocks are indicated by solid vertical lines and the boundaries of magnetic clouds or ejecta by dashed vertical lines. In the top part of each panel we indicate by vertical arrows the main CMEs and flares as pointed out by BPR, SGD, and LASCO observations. Table 1 lists the characteristics of these solar events considered as possible sources of energetic particles. The first six columns display the following: the time of maximum emission from X-ray flares, their X-ray classification, the active regions (AR) associated with the Hα emission, their location on the disk (latitude and longitude), and the reference where this information can be found. The next four columns show the characteristics of the CMEs: time, direction of propagation, angular width ω, and speed v_{CME} (indicated by asterisk when the source of information is MLSO). Association between solar flares and CMEs is based on previous studies (quoted in the last column of Table 1) and/or on their temporal and spatial coincidence. Those CMEs propagating away from the west (east) limb of the Sun are associated with flares from western (eastern) longitudes. Those solar events located on the back of the Sun are based on the reference indicated in the sixth column. For each time interval we have numbered the SEP events observed at Wind (Figures 3–8, top). The eleventh column shows the associations between the origin of those SEP events and specific solar events; the last column lists the previous works where these associations can be found.

The bottom panels of Figures 3–8 are snapshots of the spatial configuration of the Sun and of the Ulysses and Wind spacecraft as seen from the north ecliptic pole in a coordinate system fixed with respect to the Sun-Earth line. Black dots indicate the position of both spacecraft during the whole time interval plotted in the two top panels (specified in days of the year). Two nominal IMF lines (solid lines) connecting the Wind and Ulysses spacecraft to the Sun have been plotted assuming a Parker spiral. We also show a schematic representation of the corotation effect by plotting different nominal magnetic field lines (dashed field lines) rooted at the region of the Sun where Ulysses would be connected on the day indicated by the number adjacent to each field line. We assume a constant value for the solar wind speed representative of the value observed by both spacecraft (indicated in the caption of each figure), and a rotation of the Sun of 13.5°/day. The time of each snapshot is indicated by the number adjacent to the IMF line (solid line) connecting Ulysses with the Sun (plotted as a big solid circle in the center). The arrows indicate the direction (longitude) of several solar events occurring on the following days (as indicated in the text). In some panels a schematic representation of CME-driven shocks has been overplotted assuming a segment of circle propagating radially from the Sun at constant speed. In the case of reliable association between the interplanetary shock observed by one of the two spacecraft and a solar event, we assume a constant propagation speed equal to the average transit speed of the shock to travel from the Sun to the spacecraft. The width given to the shocks in these sketches (usually 180°) is only an indication of the area of heliosphere that, in principle, they may be able to fill. For simplicity, we have not plotted the distortion of the IMF lines in the downstream region of the shocks. *Lario et al.* [1999a] provide an image of the expected IMF configuration in the downstream region of traveling interplanetary shocks.

We discuss the individual periods in chronological order. The title of the following sections refers to the period of time under study. Dates are indicated throughout the paper by the number of day of the corresponding year followed by the universal time. We first present the proton observations at 1 AU. We have not included an exhaustive description of each one of the particle flux enhancements observed by Wind; instead, we have focused our study only on those intense high-energy ($\gtrsim$5 MeV) proton onsets at 1 AU with features of an SEP event (numbered in the top panels of Figures 3–8). Detailed analyses for some of these SEP events can be found in the quoted references. In order to determine those solar events associated with the origin of SEP events at 1 AU, we have considered the following factors: (1) the most intense SEP events above ~1 MeV come from solar events occurring at western longitudes or near the Central Meridian [*Cane et al.*, 1988]; (2) those SEP events associated with strong interplanetary shocks are most probably associated with solar events from near Central Meridian and driven by Earth-directed CMEs [*Cane et al.*, 1987]; (3) the shape of the proton flux profile for an SEP event at 1 AU (West-, East-, or Central Meridian-type) is a function of the location of the solar event

Table 1. Reported Solar Events Relevant to the Studied Particle Events

X-ray Flare		Hα Flare Location				CME				SEP	
Day/UT	Class	AR	Latitude	Longitude	Reference	Day/UT	Type	ω	v_{CME}, km s^{-1}	Event at Wind	References
					November 1997, Figure 3						
307/0910	M1.4	8100	S20°	W15°	SGD (no. 640, 1997)	···	···	···	···	1	1
307/1029	M4.2	···	···	···	SGD (no. 640, 1997)	307/1111	W	195°	369	1	1
308/0558	X2.1	8100	S14°	W33°	SGD (no. 640, 1997)	308/0610	halo	360°	830	$2^{\Delta\bullet}$	1, 2, 3, 4, 5
310/1155	X9.4	8100	S18°	W63°	SGD (no. 640, 1997)	310/1210	W	135°	1560	$3^{\Delta\bullet}$	1, 2, 3, 4, 5, 6
···	···	···	···	···		315/1737	E	185°	412		
···	···	···	···	···		317/2225	W	310°	449	4	1
318/1038	C4.6	8108	N21°	E70°	SGD (no. 640, 1997)	318/1014	E	75°	1127		
···	···	···	···	···		318/1336	W	240°	815	4	
319/2246	M1.0	8108	N20°	E64°	SGD (no. 640, 1997)	319/2327	E	63°	617		
···	···	···	···	···		321/0827	halo	360°	767		
323/1910	C1.6	8108	N20°	E09°	SGD (no. 640, 1997)	data gap in LASCO and MLSO					5
					April–May 1998, Figure 4						
···	···	8179	···	~E157°	BPR (no. 1179, 1998)	90/0612	halo	360°	2080		7
···	···	8179	···	~E139°	BPR (no. 1179, 1998)	91/1310	E	25°	533	1	
···	···	8179	···	~E97°	BPR (no. 1179, 1998)	94/1541	E	34°	543	1	
95/1639	M1.0	8194	S20°	E84°	SGD (no. 645, 1998)	···	···	···	···	1	
···	···	···	···	···		96/0504	W	49°	912	1	
96/1648	M1.1	8194	S30°	E78°	SGD (no. 645, 1998)	···	···	···	···	1	
···	···	···	···	···		98/0327	E	46°	564	1	
···	···	···	···	···		98/1841	W	52°	696	1	
···	···	···	···	···		100/0155	E	48°	465		
···	···	···	···	···		102/1255	E	153°	623		
···	···	···	···	···		103/0426	E	145°	495		
···	···	···	···	···		104/0526	E	81°	1188		
110/1021	M1.4	8194	···	~W125°	BPR (no. 1182, 1998)	110/1007	W	264°	1638	$2^{\Delta\bullet}$	4, 5, 6, 7, 8
113/0555	X1.2	8210	···	~E105°	BPR (no. 1182, 1998)	113/0527	halo	360°	1390		
114/0852	C8.9	8210	···	~E91°	BPR (no. 1182, 1998)	114/0855	E	61°	1245		
117/0920	X1.0	8210	S16°	E50°	SGD (no. 645, 1998)	117/0856	halo	360°	1631	$3^{\Delta\bullet}$	
119/1637	M6.8	8210	S18°	E20°	SGD (no. 645, 1998)	119/1658	halo	360°	1016	$4^{\Delta\bullet}$	
···	···	···	···	···		121/0058	E	39°	769		
121/1258	M1.1	8214	N25°	E40°	SGD (no. 646, 1998)	data gap in LASCO and no activity seen by MLSO					
121/2254	M1.2	8214	N25°	E35°	SGD (no. 646, 1998)	121/2340	halo	360°	632		
···	···	···	···	···		122/0531	halo	360°	452		
122/1342	X1.1	8210	S15°	W15°	SGD (no. 646, 1998)	122/1406	halo	360°	1044	$5^{\Delta\bullet}$	4, 5, 6
···	···	···	···	···		123/1029	W	85°	526		
123/2124	M1.4	8210	S13°	W34°	SGD (no. 646, 1998)	123/2202	W	240°	639		
125/2341	M2.5	8210	S16°	W60°	SGD (no. 646, 1998)	126/0002	W	275°	840		
···	···	···	···	···		126/0228	E	76°	511		
126/0809	X2.7	8210	S11°	W65°	SGD (no. 646, 1998)	126/0804	W	185°	1053	6^{Δ}	4, 5, 6, 9
···	···	···	···	···		127/0130	E	64°	390		
127/1114	M2.9	8214	N29°	W47°	SGD (no. 646, 1998)	···	···	···	···		
127/1342	M1.3	8214	N28°	W47°	SGD (no. 646, 1998)	···	···	···	···		
128/0608	M1.4	···	···	···	SGD (no. 646, 1998)	128/0627	W	59°	1412		
···	···	···	···	···		128/2310	E	80°	706		
129/0340	M7.7	8210	···	~W103°	BPR (no. 1184, 1998)	129/0335	W	143°	1726	7^{Δ}	5, 6
					June 1998, Figure 5						
···	···	···	···	W+	EIT images	155/0204	halo	360°	1717	1	
···	···	···	···	W+	EIT images	155/2100	W	39°	517	1	
···	···	···	···	E+	EIT images	155/2127	E	59°	652	1	
155/2205 ↔ 156/1036	FD	···	S29°	W11°	BPR (no. 1190, 1998)	156/0702	W	114°	755	1	
156/0548	FD	···	S39°	E05°	SGD (no. 652 (II), 1998)	···	···	···	···		
156/0548	FD	···	S41°	W18°	SGD (no. 652 (II), 1998)	···	···	···	···		
···	···	···	···	E+	EIT images	156/1201	halo	360°	412		
···	···	···	···	E+	EIT images	158/0932	halo	360°	516		
162/1027	M1.4	···	···	···	SGD (no. 647, 1998)	162/1028	E	156°	1312		
164/0419	M1.9	8242	S27°	E54°	SGD (no. 647, 1998)	164/0526	E	51°	792		
···	···	···	···	···		166/1727	E	86°	703		
167/1842	M1.0	8232	···	~W103°	BPR (no. 1190, 1998)	167/1827	W	252°	1650	2^{Δ}	10
···	···	···	···	E+	EIT images	171/1820	halo	360°	1038		
172/1808	C1.2	8243	N16°	W38°	SGD (no. 647, 1998)	172/1815	W	94°	822		
173/0433	C2.9	8243	N16°	W46°	SGD (no. 647, 1998)	···	···	···	···		
173/1212	FD	···	S51°	W24°	SGD (no. 652 (II), 1998)	···	···	···	···	3	
···	···	···	···	···		174/0359	W	73°	447		

Table 1. (continued)

X-ray Flare		Hα Flare Location				CME				SEP Event at Wind	References
Day/UT	Class	AR	Latitude	Longitude	Reference	Day/UT	Type	ω	v_{CME}, km s^{-1}		
					August 1998, Figure 6						
...	...	...	...	...		*228/1737	E	74°	770		
228/1821	M3.1	8307	...	~E114°	BPR (no. 1198, 1998)	...	...	...	...		
229/2120	X1.2	8307	...	~E93°	BPR (no. 1199, 1998)	*229/2116	E	36°	800		
230/0416	M1.5	8307	...	~E89°	BPR (no. 1199, 1998)	no MLSO Observations					
230/0831	X2.8	8307	N33°	E87°	SGD (no. 649, 1998)	no MLSO Observations					
230/2219	X4.9	8307	N33°	E87°	SGD (no. 649, 1998)	no MLSO Observations					
231/1241	M2.3	8307	N35°	E78°	SGD (no. 649, 1998)	no MLSO Observations					
231/1429	M3.0	8307	N35°	E80°	SGD (no. 649, 1998)	no MLSO Observations					
231/2145	X3.9	8307	N30°	E75°	SGD (no. 649, 1998)	*231/2141	E	45°	1830		
234/0009	M9.0	8307	N42°	E51°	SGD (no. 649, 1998)	no coronal activity seen by MLSO				1	
235/0931	M2.2	8307	N32°	E33°	SGD (no. 649, 1998)	no MLSO Observations				1	
236/2212	X1.0	8307	N35°	E09°	SGD (no. 649, 1998)	Earth-directed CME not observed by MLSO				2	4, 5, 6, 8
242/0541	M1.0	8319	N21°	W33°	SGD (no. 649, 1998)	no MLSO Observations					
242/0937	M1.3	8319	N21°	W35°	SGD (no. 649, 1998)	no MLSO Observations					
243/1539	M1.5	8307	N32°	W69°	SGD (no. 649, 1998)	no MLSO Observations					
244/0459	M1.5	8307	N32°	W78°	SGD (no. 650, 1998)	no MLSO Observations					
245/1707	M2.2	8319	N17°	W79°	SGD (no. 650, 1998)	no MLSO Observations					
246/0412	M1.3	8326	N20°	E90°	SGD (no. 650, 1998)	no MLSO Observations					
246/1430	C3.9	8323	S20°	E05°	SGD (no. 650, 1998)	no MLSO Observations					
246/1608	M1.1	8323	S20°	E06°	SGD (no. 650, 1998)	no coronal activity seen by MLSO					
252/0458	M2.8	8323	S22°	W65°	SGD (no. 650, 1998)	no coronal activity seen by MLSO				4	
					September–October 1998, Figure 7						
266/0713	M7.1	8340	N18°	E09°	SGD (no. 650, 1998)	no MLSO observations				1	11
271/0654	M3.5	...	...	...	SGD (no. 650, 1998)	...	...	...			
...	...	...	...	...		*271/1907	W	...	too faint		
273/1338		8346	S28°	W35°	SGD (no. 650, 1998)	no coronal activity seen by MLSO				2	5, 6
273/1434	M2.8	8340	N23°	W81°	SGD (no. 650, 1998)	no coronal activity seen by MLSO				2	5, 6
280/1247	M1.6	8355	S22°	E68°	SGD (no. 651, 1998)	...	...	...	...		
280/1712	M2.3	8355	S20°	E65°	SGD (no. 651, 1998)	*280/<1747	E	11°	too faint		
287/1704 ↔ 288/1101	FD	...	N19°	E10°	SGD (no. 656 (II), 1999)	288/1004	halo	360°	230	3	
291/0145	M2.4	8358	N16°	W52°	SGD (no. 651, 1998)	no LASCO, MLSO observations					
293/2103	C7.4	...	...	...	SGD (no. 651, 1998)	no LASCO, MLSO observations					
					November 1998, Figure 8						
308/0337	C5.2	8375	N17°	E01°	SGD (no. 652, 1998)	308/0418	halo	360°	607		
...	...	...	...	...		309/0241	halo	360°	435		
309/1335	M1.5	8375	N15°	W17°	SGD (no. 652, 1998)	...	...	...	...		
309/1955	M8.4	8375	N22°	W18°	SGD (no. 652, 1998)	309/2044	halo	360°	910	1$^{\Delta\bullet}$	12
310/1511	M1.7	8375	N15°	W32°	SGD (no. 652, 1998)	...	...	...	...		
311/1106	M2.4	...	...	...	SGD (no. 652, 1998)	...	...	...	...		
...	...	...	...	...		311/2118	W	99°	624		
312/1712	M2.7	8375	N19°	W58°	SGD (no. 652, 1998)	...	...	...	...		
312/2256	M1.1	8375	N21°	W61°	SGD (no. 652, 1998)	...	...	...	...		
...	...	...	...	...		313/0725	E	76°	754		
313/1535 ↔ 1717	FD	...	N17°	W90°	SGD (no. 657 (II), 1999)	313/1754	W	178°	327		
...	...	...	...	...		313/2054	W	57°	661		
314/1544	M1.8	8375	N23°	W77°	SGD (no. 652, 1998)	314/1418	W	117°	643		
315/0407	M1.0	...	...	...	SGD (no. 652, 1998)	...	...	...	...		
315/1016	M1.1	...	...	...	SGD (no. 652, 1998)	...	...	...	...		
316/0528	M1.0	8385	N21°	W34°	SGD (no. 652, 1998)	...	...	...	...		
318/0508	C1.3	8375	...	~W117°	BPR (no. 1211, 1998)	no LASCO, MLSO observations				2	5, 6, 12
318/0519	C1.7	8385	N20°	W60°	SGD (no. 652, 1998)	no LASCO, MLSO observations				2	5, 6
320/2153	C4.9	8383	S14°	W29°	BPR (no. 1212, 1998)	no LASCO, MLSO observations					
326/0642	X3.7	8384	S27°	W82°	SGD (no. 652, 1998)	no LASCO, MLSO observations					
326/1623	X2.5	8384	S30°	W89°	SGD (no. 652, 1998)	no LASCO, MLSO observations					
327/0644	X2.2	8384	S28°	W89°	SGD (no. 652, 1998)	no LASCO, MLSO observations					
328/0220	X1.0	8384	...	~W99°	BPR (no. 1213, 1998)	328/0230	halo	360°	1681		
...	...	...	...	...		330/0254	halo	360°	1166		
331/0743	M1.6	8392	S24°	E09°	SGD (no. 652, 1998)	...	...	...	...		
...	...	...	...	...		331/1830	W	94°	473		
332/0609	X3.3	8395	N17°	E32°	SGD (no. 652, 1998)	332/0630	E	236°	805		

1, *Mäkelä et al*. [1999]; 2, *Lario et al*. [1998a]; 3, *Mason et al*. [1999]; 4, *Timofeev and Starodubtsev* [1999]; 5, *von Rosenvinge et al*. [1999]; 6, *Dietrich and Lopate* [1999]; 7, *Marsden et al*. [1999]; 8, *Tylka et al*. [1999]; 9, *McKenna-Lawlor et al*. [1999]; 10, *Torsti and Sahla* [1999]; 11, *Richardson and Cane* [1999]; 12, *Lario et al*. [1999b]. SGD, Solar-Geophysical Data; BPR, Boulder Preliminary Reports.

responsible for its origin [*Cane et al*., 1988]; and (4) there is a close association between fast CMEs ($v_{CME} \geq 400$ km s^{-1}) and intense SEP events at 1 AU. The higher the speed of an optimally located CME, the higher is the probability of an accompanying SEP event at 1 AU [*Kahler et al*., 1999]. From this analysis we obtain the main solar events able to populate those parts of the heliosphere scanned by Wind. By comparing the times of CMEs and X-ray flares with the onset of the proton events at 1 AU, as well as the shape of the proton flux profiles with the heliolongitude of the solar events, we specify those solar events related to the origin of SEP events at Wind. However, there are other solar events that cannot be associated with SEP events at 1 AU, mainly due to their poor magnetic connection (CMEs propagating away from the east limb of the Sun) or the fact that they occurred when the Wind flux profile was dominated by a previous SEP event and we cannot determine their actual contribution to the proton flux. These solar events have also been considered in Table 1 as potential sources of particles for an SEP event at Ulysses. On the other hand, those CMEs propagating away from the west limb of the Sun, in principle well connected to Wind, but which did not produce a proton flux enhancement at this spacecraft (i.e., during periods of quiet flux profiles), are not included in Table 1 because of their supposed inefficiency in particle acceleration. The observation at Ulysses of the effects of these solar events will depend on its location and on the extent and efficiency of the associated shocks.

3.1. November 1997

Figure 3 shows Wind and Ulysses observations as well as their respective locations from day 307 to day 333 of 1997. The particle events observed during this period constituted the first intense high-energy particle events observed by both spacecraft in the rising phase of the solar cycle 23 and they have been widely studied [*Lario et al*., 1998a; *Mason et al*., 1999; *Timofeev and Starodubtsev*, 1999]. These studies focused on the particle effects due to the CMEs occurring on days 308 and 310; there are, however, many other solar events occurring throughout the period of Figure 3 (Table 1) which must be considered as potential sources of particles filling the heliosphere and observed by Wind and Ulysses.

3.1.1. Wind observations. Wind observed five different SEP events during this period (as numbered in Figure 3a). The onset of the first proton flux enhancement was detected by Wind at 307/1300 UT in coincidence with a change of the magnetic field orientation. This proton event was observed only at high energies (>0.8 MeV) and had a very short duration (~17 hours). *Mäkelä et al*. [1999] relate the origin of this proton event to a slow CME observed at 307/1111 UT propagating away from the west limb. There were two X-ray flares around the time of this CME: the first at 307/0910 UT from S20°W15° and the second at 307/1029 UT with no optical association on the solar disk (Table 1). Only the high-energy protons injected from these solar events were able to reach Wind before a new particle population associated with SEP event number 2 arrived at this spacecraft. This new injection has been associated with a halo CME at 308/0610 UT [*Lario et al*., 1998a] which was able to drive an interplanetary shock arriving at Wind at 310/2219 UT. The average shock transit speed to travel from the Sun to Wind was $\langle v \rangle \simeq 646$ km s^{-1}. This shock was followed by a magnetic cloud 7 hours later (dashed lines in Figure 3a) that we interpret as the interplanetary counterpart of the CME.

A fast CME propagating away from the west limb at 310/1210 UT generated SEP event number 3 at Wind (see *Lario et al*. [1998a] for details). *Reiner et al*. [1998] interpreted the arrival of a weak shock at Wind at 313/1003 UT as the east flank of the shock driven by this CME when arriving at Wind. This implies an average shock transit speed of $\langle v \rangle \simeq 590$ km s^{-1}. Using type II radio emissions and considering a value for the solar wind density as measured by Wind at that moment, *Reiner et al*. [1998] infer a shock speed above the active region (S18°W63°) of ~1000 km s^{-1}, which was significantly faster that the shock speed in the direction to Wind. The higher solar wind density presumably existing above the active region (located in the downstream medium of the previous interplanetary shock) would lead to a higher shock speed above the active region. There is no clear contribution of this shock to the proton flux when it arrived at Wind. Nevertheless, the increase of flux observed shortly after the occurrence of the CME suggests that the shock was very efficient accelerating particles nearer the Sun. At high energies ($\gtrsim$5 MeV) this SEP event had a typical profile of a West-type event. In this type of event the observer is initially connected to the nose of the CME-driven shock and shock-accelerated particles quickly reach the spacecraft (in a few minutes depending on their energy). As the shock expands, only the weak east flank of the shock arrives at the spacecraft; this part of the shock front is less efficient at accelerating particles [*Heras et al*., 1995], thus giving a much smaller contribution to the proton flux. In the decaying phase of this SEP event, there is a simultaneous decrease of the proton intensities at 313/2205 UT in all energy channels. It coincides with the arrival of a weak interplanetary shock associated with a discontinuity of the IMF which represents a change of the flux tube in which Wind was located.

At the end of day 317 a new SEP event (number 4) was observed at Wind; it had the profile of a West-type event but less intense than the SEP event number 3 and without the arrival of any associated shock. *Mäkelä et al*. [1999] associate this event with the CME at 317/2225 UT observed propagating away from the west limb of the Sun (Table 1). Another CME at 318/1336 UT was also observed propagating away from the west limb which, in principle, could also contribute to the proton flux observed by Wind. During the development of this SEP event, two new CMEs occurred at the east limb of the Sun (Table 1). None of them generated an SEP event at Wind due to its poor magnetic connection to eastern longitudes. A spiky proton flux enhancement (number 5 in Figure 3) was observed in association with a strong forward shock arriving at Wind at 326/0912 UT and followed by a magnetic cloud 5 hours later. We associate this proton flux enhancement, a so-called "energetic storm particle" (ESP) event, with a population of particles locally accelerated by the shock which remained trapped around its front. The origin of this shock is probably an Earth-directed CME occurring at the same time as a long-duration flare from N20°E09° (BPR, no. 1160, 1998). The lack of LASCO and MLSO observations during this period does not allow us to associate this shock with any reported CME; however, assuming that a CME occurred simultaneously with the flare, the associated driven shock would have been traveling to Wind at $\langle v \rangle \simeq 670$ km s^{-1}.

3.1.2. Ulysses observations. Proton flux observations at Ulysses show a long-lasting (more than 25 days) particle event. Proton-to-alpha ratios [*Sanderson et al*., 1999, Figure 3] suggest that particles observed during this period are SEP event related. *Lario et al*. [1998a] describe in detail the Ulysses obser-

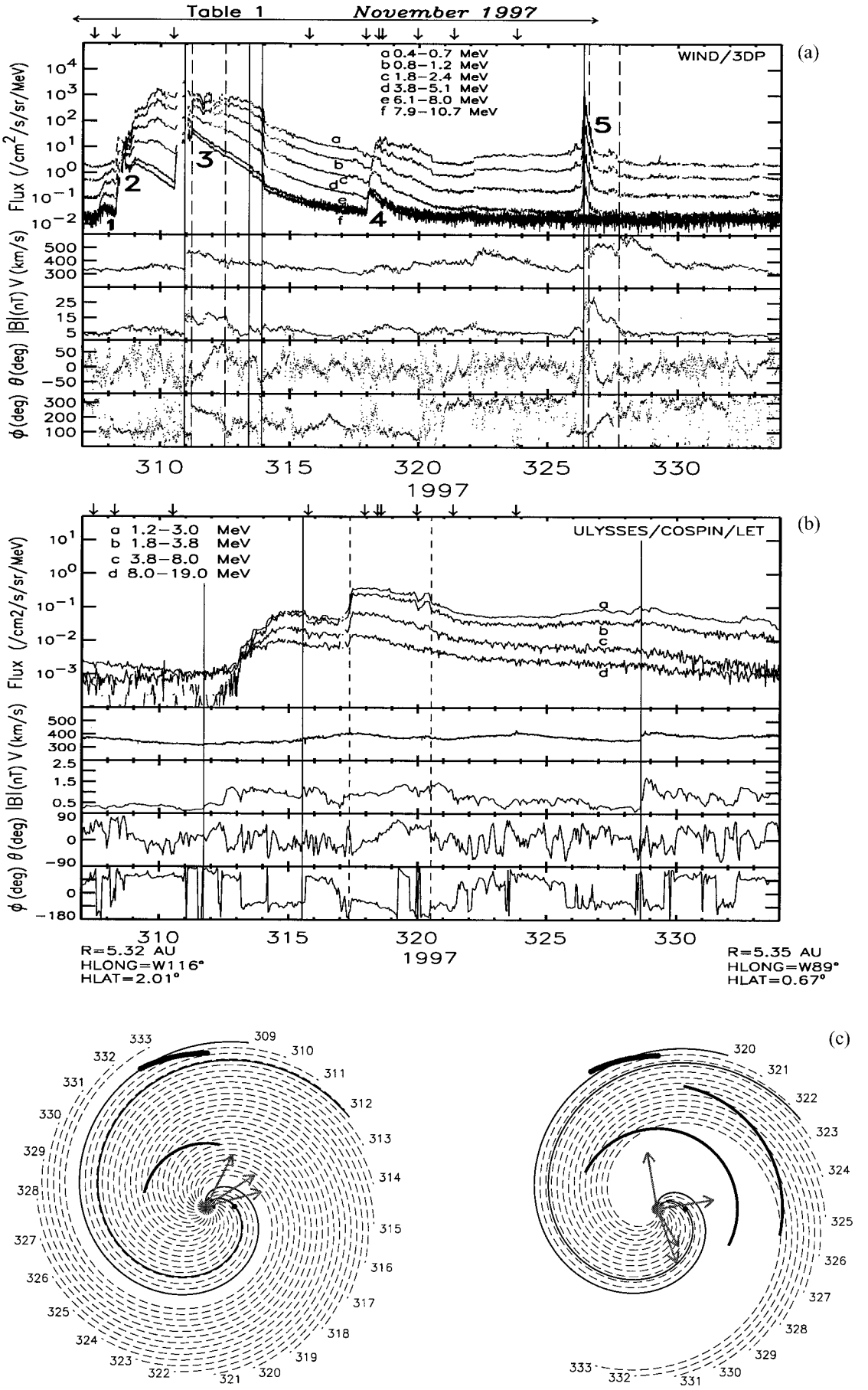

Figure 3. (a) Wind and (b) Ulysses observations for the November 1997 period; (c) spatial configuration of the ecliptic plane on (left) day 309 and (right) day 320 assuming a solar wind speed of 350 km s^{-1}. See text for details.

vations for this period. The main arrival of particles was observed in association with a sector boundary crossing on day 313. A weak forward shock was observed at 315/1225 UT followed by a magnetic cloud with a high proton intensity arriving at Ulysses at 317/0830 UT. A forward shock was observed at 328/1508 UT with a contribution to the low-energy (<3.8 MeV) proton flux. The proton flux profile did not decrease to background levels until well into December 1997. An electron flux enhancement was observed by Ulysses in association with this event (Figure 2). The onset of the electron flux was observed above the instrumental background on day 311 and reached a maximum at the beginning of day 314 when proton fluxes were still increasing. According to the nominal IMF structure (Figure 3, bottom) Ulysses was connected to the west limb of the Sun. Taking into account the prompt arrival of these electrons, we suggest that Ulysses was connected to regions close where the CME at 310/1210 UT took place. The main arrival of protons at Ulysses was due to the acceleration effects of a shock driven by this CME. Wind observations suggest that the halo CME at 308/0610 UT was also able to drive a strong shock front that was a very active particle accelerator when it was close to the Sun. Energetic protons accelerated by this shock propagated along those field lines which established magnetic connection with Ulysses from day 312 onward (Figure 3, left bottom). The arrival of these particles together with the main contribution of particles from the CME at 310/1210 UT constituted the SEP event observed at Ulysses (see *Lario et al*. [1998a] for details).

Lario et al. [1998a] interpret the arrival of shocks and magnetic clouds at Ulysses and Wind in terms of the CMEs on days 308 and 310. They suggest a possible scenario where the shock observed by Ulysses at 315/1225 UT was related to the CME at 310/1210 UT [*Lario et al*., 1998a, Figures 1 and 4]. The shock driven by this CME would have propagated at $\langle v \rangle \simeq 1800$ km s^{-1} in the direction to Ulysses. In this scenario the forward shock observed by Ulysses at 328/1508 UT was driven by the CME at 317/2225 UT propagating to the west with $\langle v \rangle \simeq 864$ km s^{-1}. In principle, the effects of a fast shock ($\sim$1800 km s^{-1}) propagating through an interplanetary medium characterized by a solar wind speed of 350 km s^{-1} (as observed by Ulysses in the upstream region of the shock) would give a discontinuity of the solar wind and magnetic field parameters bigger than observed. This could argue against the proposed scenario; nevertheless, the lack of solar events at the end of October 1997 and beginning of November 1997 complicates the association of the shock and magnetic cloud with a specific solar event.

As alternative, we suggest that a narrow CME ($\omega = 54°$, $v_{\mathrm{CME}} = 646$ km s^{-1}), observed by LASCO at 304/0930 UT propagating away from the west limb, was well directed toward Ulysses to produce the shock observed at 315/1225 UT ($\langle v \rangle \simeq 828$ km s^{-1}) and the subsequent magnetic cloud. There is no reported solar flare or filament disappearance in temporal association with this CME (Solar Geophysical Data, no. 639, 1997). The downstream region of this shock (including the magnetic cloud) would have been filled with energetic particles coming from the CMEs on days 308 and 310. Figure 3 (left bottom) shows the shock front driven by the CME at 304/0930 UT as it travels to Ulysses with a speed of 828 km s^{-1}, the three arrows indicate the longitude of the three successive CMEs occurring on days 307, 308, and 310 and producing the SEP events number 1, 2, and 3 at Wind, respectively. The shock observed by Ulysses at 328/1508 UT would probably be associated with the western CME at 310/1210 UT (that means $\langle v \rangle \simeq 510$ km s^{-1}). Figure 3 (right bottom) shows the shock fronts associated with the CME on day 308 (directed to the Earth at 646 km s^{-1}) and with the CME on day 310 (directed to Ulysses at 510 km s^{-1}). The four arrows indicate the longitude of the next solar events (Table 1) occurring at 317/2225 UT (from the west limb but without any flare associated on the solar disk), 318/1014 UT (E70°), 319/2327 (E64°), and 323/1700 (E09°), which filled the heliosphere with energetic particles and contributed to extend the duration of the SEP event at Ulysses. It is important to note that these solar events and the related shocks were able to inject particles not only on to the field line connected to Ulysses at the time of their occurrence but also on to those field lines (dashed lines in Figure 3c) that, by the corotation effect, were connected to Ulysses some days later. In this alternative scenario, the CME at 317/2225 UT did not produce any strong shock able to reach Ulysses and to produce a significant proton flux enhancement as Wind observations seem to indicate.

3.2. April–May 1998

3.2.1. Wind observations. Figure 4a shows Wind observations from day 90 to day 141 of 1998. We distinguish three main periods in Wind particle observations: a proton flux enhancement from day 94 to day 105 with a relatively high proton intensity in all energy channels (event number 1); a long-lasting SEP event from day 110 to day 116 (event number 2); and a sequence of intense proton flux increases from day 116 to day 132 (numbered from 3 to 7 in Figure 4a).

The proton flux enhancement number 1 showed a gradual increase from 94/$\sim$1300 UT, it reached a maximum at the end of day 97 and slowly decayed until day 105. The evolution was similar in all energy channels indicating a long-lasting period of constant spectrum. Table 1 includes the main solar events occurring from day 90 onward. A very fast halo CME was observed on day 90. Its origin was associated with AR 8179 located on the back of the Sun (Boulder Preliminary Reports, no. 1179, 1998). Taking into account that this region crossed the west limb at the end of day 81, at the time of the CME it was at $\sim$E157°. Two additional CMEs were also detected above the southeast limb at 91/1310 UT and 94/1541 UT, and probably associated with the same region AR 8179 (BPR, no. 1179, 1998). When this active region returned to the visible disk, it was assigned the number AR 8194 and produced two new solar flares on day 95 and 96. Several CMEs, without any associated classic solar event (flare, FD), were also detected from day 96 to 104 (Table 1). Figure 4c (left) shows the interplanetary configuration on day 90 when the CME at 90/0612 UT took place; the arrow indicates the longitude of its solar origin, which was located far away from the root of the magnetic field line connecting to Wind. In principle, energetic particles injected directly from the CME site, and from the other eastern solar events occurring between days 91 and 104, are not expected to be observed by Wind. However, an interplanetary shock expanding out from the east limb of the Sun may, at some stage during its propagation (beyond 1 AU), leave Wind behind it. In this situation, Wind establishes magnetic connection to the downstream region of the shock. Energetic particles contained in this region, and probably accelerated by the same shock, are then available to be observed by Wind. The constant spectrum observed from day 94 to day 105 is characteristic of the downstream region of traveling interplanetary shocks [*Reames et al*., 1997]. However, no typical SEP event profile (West-, East-, or Central Meridian) can be

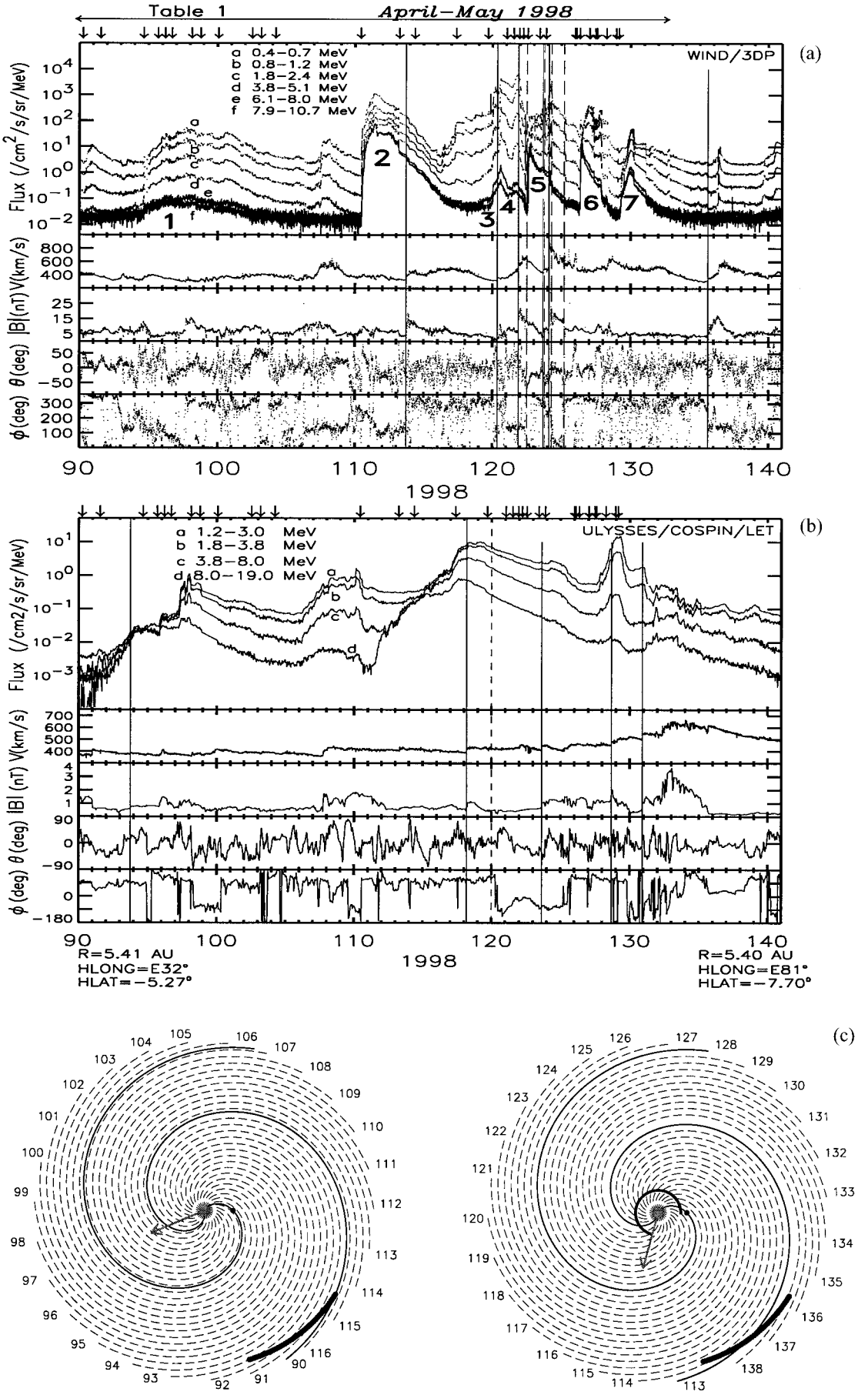

Figure 4. (a) Wind and (b) Ulysses observations for the April–May 1998 period: (c) spatial configuration of the ecliptic plane on (left) day 90 and (right) day 113 assuming a solar wind speed of 400 km s^{-1}. See text for details.

distinguished in the proton flux enhancement number 1. We suggest that the backside eastern CMEs on days 90, 91, and 94 contributed in some way to this proton flux enhancement.

Wind detected a large proton flux onset at 110/1140 UT; with an increase of the 7.9–10.7 MeV proton intensity of more than 3 orders of magnitude in less than four hours. The profile and evolution of this particle event is characteristic of a West-type SEP event. It was associated with the arrival of an interplanetary shock at 113/1730 UT. The origin of this SEP event has been identified with a CME at 110/1007 UT [*Tylka et al*., 1999]. A long-duration M1.4 flare, without Hα identification, was observed around the same time (Solar-Geophysical Data, no. 645, 1998). The peak X-ray intensity observed on Yohkoh during this period was at S23°W87° [*Tylka et al*., 1999]; however, according to Boulder Preliminary Report (no. 1182, 1998) the source was likely the old AR 8194 which at the time of the CME was located 2.5 days behind the southwest limb (~W125°). The CME-shock association implies $\langle v \rangle \simeq 526$ km s^{-1}, which is a reasonable value for the east flank of a shock generated from western longitudes and arriving at 1 AU.

The decay phase of the SEP event number 2 lasts until day 116 when a sequence of new SEP events were observed (events number 3–7 in Figure 4). From day 113, solar activity increased to high levels mainly due to the active region AR 8210; its presence in the visible disk (from day 114 to 128) was characterized by a continuous production of CMEs and flares (Table 1). Moreover, it was preceded by flares even when the region was behind the east limb and followed by other solar flares even when it was behind the west limb of the Sun (Boulder Preliminary Report, no. 1182–1184, 1998). Each one of these solar events had different effects on the proton flux at Wind depending on the location of AR 8210 with respect to Wind. All flux profiles described in Figure 15 of *Cane et al*. [1988] (West-, East-, Central Meridian-type) are observed during this period; but in this case, all the different types of SEP events were generated by the same active region as it changed its location with respect to the observer.

On days 113 and 114 AR 8210 was located behind the east limb of the Sun, and their contribution to Wind flux profiles remained masked below the SEP event number 2. As AR 8210 approached the Central Meridian, CME-driven shocks reached Wind and produced distinguishable SEP events. We associate the CME from E50° at 117/0856 UT with the East-type particle event number 3, which was associated with a shock arriving at Wind at 120/0840 UT ($\langle v \rangle \simeq 582$ km s^{-1}). It is worth pointing out that the maximum of proton flux at low-energies for this particle event occurred at the time of the shock arrival, but at high energies the maximum occurred several hours later. This is a typical feature of East-type events and suggests that the observer establishes magnetic connection to strong regions of the shock front as the shock moves beyond the observer location [see *Lario et al*., 1999a]. A new halo CME from E20° generated the particle event number 4 that superimposed on the decaying phase of the previous event. A shock at 121/2120 UT ($\langle v \rangle \simeq 788$ km s^{-1}) followed by a magnetic cloud 14 hours later are the interplanetary effects of this CME at Wind. The SEP event number 5 was associated with the halo CME from W15° at 122/1406 UT [*von Rosenvinge et al*., 1999]. The particles accelerated by the CME-driven shock arrived at Wind when the magnetic cloud from the previous event was crossing this spacecraft. The presence of this cloud modified the free propagation of low-energy protons which scarcely reached Wind, but higher-energy protons produced an SEP event of West-type profile at Wind. Low-energy proton flux peaked with the arrival of an interplanetary shock at 123/1610 UT which we interpret as being driven by the CME from W15° ($\langle v \rangle \simeq 1570$ km s^{-1}). It is important to point out that this shock arrived at Wind before the trailing edge of the magnetic cloud from the previous event. At 124/0225 UT a strong interplanetary shock arrived at Wind, followed by a solar wind of very high speed (>900 km s^{-1}). Signatures of ejecta were found between 124/~0700 UT and 125/~0500 UT, which can be interpreted as the interplanetary counterpart of the CME from W15° that generated the SEP event number 5.

When AR 8210 was located at western longitudes (day ~125), the associated CMEs did not produce interplanetary shocks at Wind. The fact that only the weak east flank of these shocks could reach Wind and the fact that these CMEs propagated through the disturbed downstream medium left by the previous shocks, make its detection difficult, or even might prevent the formation of their flanks which may dissipate as they propagate through the interplanetary medium. In addition, the high solar wind speed observed between the two ejecta (on day 124) seems to impede the CME at 123/2202 UT from W34° to form an interplanetary shock strong enough to be observed by Wind. Finally, the CMEs from W65° and ~W103° have been associated with the West-type SEP events number 6 and 7 (see *Dietrich and Lopate* [1999], *von Rosenvinge et al*. [1999], and *Mckenna-Lawlor et al*. [1999] for details). Solar events on days 127 and 128 (Table 1) occurred in the decaying phase of the SEP event number 6, and their actual contribution to the proton flux cannot be determined.

3.2.2. Ulysses observations. The sequence of CMEs throughout April and May 1998 yields to a completely different flux profile at Ulysses. *Marsden et al*. [1999] report Ulysses observations during this period and suggest a possible scenario in terms of the activity occurring at the Sun; we refer to this work for further details. A first proton onset showing features of velocity dispersion occurred on day 90; *Marsden et al*. [1999] associate it with the fast halo CME on day 90, which started propagating near the foot point of the IMF line connecting Ulysses. Figure 4c (left) shows the magnetic connection between Ulysses and the Sun on day 90. High-energy electron intensity, however, did not show a significant increase at that time (Figure 2), suggesting that magnetic connection between Ulysses and the site of the active region generating this event was not directly established, or that this solar event was not efficient enough to accelerate electrons at these energies. We suggest that a wide shock driven by the CME on day 90 injected energetic protons on to those IMF lines connecting to Ulysses generating the first SEP event at this spacecraft. Eastern solar events from day 91 to 104 (with solar sites close to the root of the IMF lines connecting to Ulysses) contributed to extend the SEP event at Ulysses. Using 1.3–2.2 MeV proton data from the Anisotropy Telescopes of the COSPIN instrument on board Ulysses [*Simpson et al*., 1992], *Dalla and Balogh* [2000] compute flow anisotropies for this period showing a strong streaming of protons coming directly from the Sun that supports our suggested scenario.

The Ulysses proton flux enhancement observed on day 111 also showed features of velocity dispersion indicating that the particles had traveled a significant way before reaching this spacecraft. Anisotropies also show a strong antisunward streaming of particles at that time [*Dalla and Balogh*, 2000]. *Marsden et al*. [1999] associate this proton increase with the CME at 110/1007 UT. The solar origin given to this CME

(~W125° according to Boulder Preliminary Reports (no. 1182, 1998), or W87° according to *Tylka et al*. [1999]) was very distant from the root of the IMF connecting with Ulysses. The shock driven by this CME was observed by Wind, which suggests a minimum width for the shock of 250° or 174°, depending on the solar origin considered. Figure 4c (right) shows the interplanetary configuration at the beginning of day 113, when the east flank of this shock (plotted assuming a constant speed of 526 km s^{-1} and a width of 250° centered at W125°) was arriving at Wind. Observation of 2.5–7.0 MeV electrons by Ulysses (Figure 2) shows an increase of flux at the end of day 110. A first maximum was reached on day 112 when proton fluxes were still increasing. At that time, the nominal Ulysses connection was established behind the east limb of the Sun, precisely where AR 8210 was located (Figure 4c). However, there are no flares or CMEs reported from that part of the Sun at that time. We suggest two possibilities to explain the origin of these prompt flux increases at Ulysses: either the CME on day 110 had an exceptional character that would have led it to accelerate and inject electrons from points very distant from the original source region, or several solar events occurred at the time of the CME on day 110 being able to fill with electrons and protons large extensions of the heliosphere.

The sequence of CMEs from AR 8210 between days 113 and 129 (Table 1) filled the heliosphere from different longitudes and at different times, producing five different SEP events at Wind. Ulysses proton observations do not allow us to distinguish the same sequence of particle events. A smooth and long-lasting particle event was observed by Ulysses from the beginning of day 111 to day 140. We suggest that the associated traveling shocks were able to continuously inject particles on to IMF lines located at different parts of the heliosphere and which successively crossed Ulysses, contributing to extend the duration of the particle event at Ulysses. It is worth pointing out that relativistic electron intensity at Ulysses registered an increase at 113/~0800 UT (not distinguishable in Figure 2 because of its compact timescale, but which was also observed at energies >7 MeV). We interpret this electron flux enhancement as the result of a direct contribution from the solar event at 113/0555 UT (Table 1) whose solar site (indicated by an arrow in Figure 4c (right)) was close to the root of the IMF line connecting to Ulysses. The later solar events from AR 8210 did not produce significant increases in the Ulysses electron flux, but the associated driven shocks contributed to the proton flux. *Marsden et al*. [1999] associate the arrival of the shocks at Ulysses at 128/1613 UT and at 130/2146 UT with the CMEs from E50° and E20°, implying average transit speeds of 830 and 836 km s^{-1} respectively. Another interplanetary shock was observed at 118/0431 UT followed by signatures of a magnetic cloud on day 120. The association of this shock with the fast eastern CME at 104/0526 UT gives $\langle v \rangle \simeq 670$ km s^{-1}. The propagation direction of these three CMEs was well oriented to produce interplanetary shocks at Ulysses, being still efficient enough to accelerate protons as shown by the observed flux enhancements on their arrival. When AR 8210 was located at Central Meridian and western longitudes (from day 122 onward), the CMEs produced from there were able to drive interplanetary shocks that, even not being well directed to Ulysses, were able to inject energetic particles on to those field lines that crossed Ulysses some days later (indicated by dashed lines in Figure 4c) and contributed to extend the period of time with high proton intensities at Ulysses.

3.3. June 1998

Figure 5 shows the Wind and Ulysses observations and their respective locations from day 155 to day 180. The nominal magnetic field connection of Ulysses with the Sun is established now on the nonvisible part of the Sun (Figure 5c). The difficulty in observing backside events complicate the identification of the proton events at Ulysses with specific solar events.

3.3.1. Wind observations. Three small proton flux enhancements were observed by Wind with onsets at 155/1130 UT, 167/~2100 UT, and 173/2330 UT (numbered 1, 2, and 3 of Figure 5a). The first proton event does not have signatures of any characteristic flux profile of an SEP event at 1 AU (West-, East-, or Central Meridian-type). It was observed just before the arrival of a high-speed (>600 km s^{-1}) solar wind stream crossing Wind on days 158–162. A fast halo CME occurred at 155/0204 UT that according to SOHO/EIT images (ftp://lasco6.nascom.nasa.gov/pub/lasco/status/) was generated from behind the visible disk of the Sun. Late on day 155, two more CMEs occurred from behind the solar disk (Table 1). We suggest that the shocks driven by these CMEs across the corona and through the interplanetary medium were very efficient accelerators of particles, as supported by Ulysses observations (see discussion below). Coronal shocks, which may have widespread extensions around the Sun [*Cliver et al*., 1995], may not only fill the part of the heliosphere located behind the Sun but also contribute to the proton flux enhancement number 1 at Wind, which because of the oscillating character of the IMF direction throughout days 156 and 157 and the contribution from the high-speed stream, shows an irregular profile. We note also that this event occurred on the decaying phase of a previous particle event observed by Wind on day 153 (not shown here), which may contribute to its irregular flux profile. Two new CMEs, the first at 156/0702 UT observed in association with three FDs early on the same day 156 (BPR, no. 1188, 1998) and the second at 156/1201 UT associated with a backside event, contributed to extending the period with high proton intensity of the SEP event number 1 until the end of day 157 when the high-speed stream arrives.

The SEP event number 2 was observed starting at 167/~2100 UT with features of velocity dispersion. *Torsti and Sahla* [1999] associate the origin of this event with a CME on the west limb at 167/1827 UT. Around the same time a M1.0 solar flare occurred. According to BPR (no. 1190, 1998) this flare was produced from the old region AR 8232 which at the time of the CME was one day behind the west limb of the Sun (~W103°). However, this SEP event did not show the typical profile of a West-type event. Proton fluxes peaked at the end of day 169 in association with a plasma and magnetic field discontinuity not classified as a shock because the increase of solar wind speed and IMF magnitude was gradual (http://lepmfi.gsfc.nasa.gov/). We point out also that the change of the IMF orientation throughout days 169 and 170 contributed to the irregular flux profile of this SEP event.

The proton event number 3 was only observed by Wind/3*DP* instrument at energies below 5 MeV. Just prior to the onset of this event, a FD developed around S51°W24° at 173/1212 UT (Table 1). A magnetic cloud arrived at Wind at 175/1400 UT. We suggest two possible origins for this cloud, either it was originated by the FD, which gives an average transit speed for the cloud of ~834 km s^{-1}; or this cloud was the interplanetary counterpart of a CME at 172/1815 UT from W38° which implies an average transit speed of ~613 km s^{-1}. From our

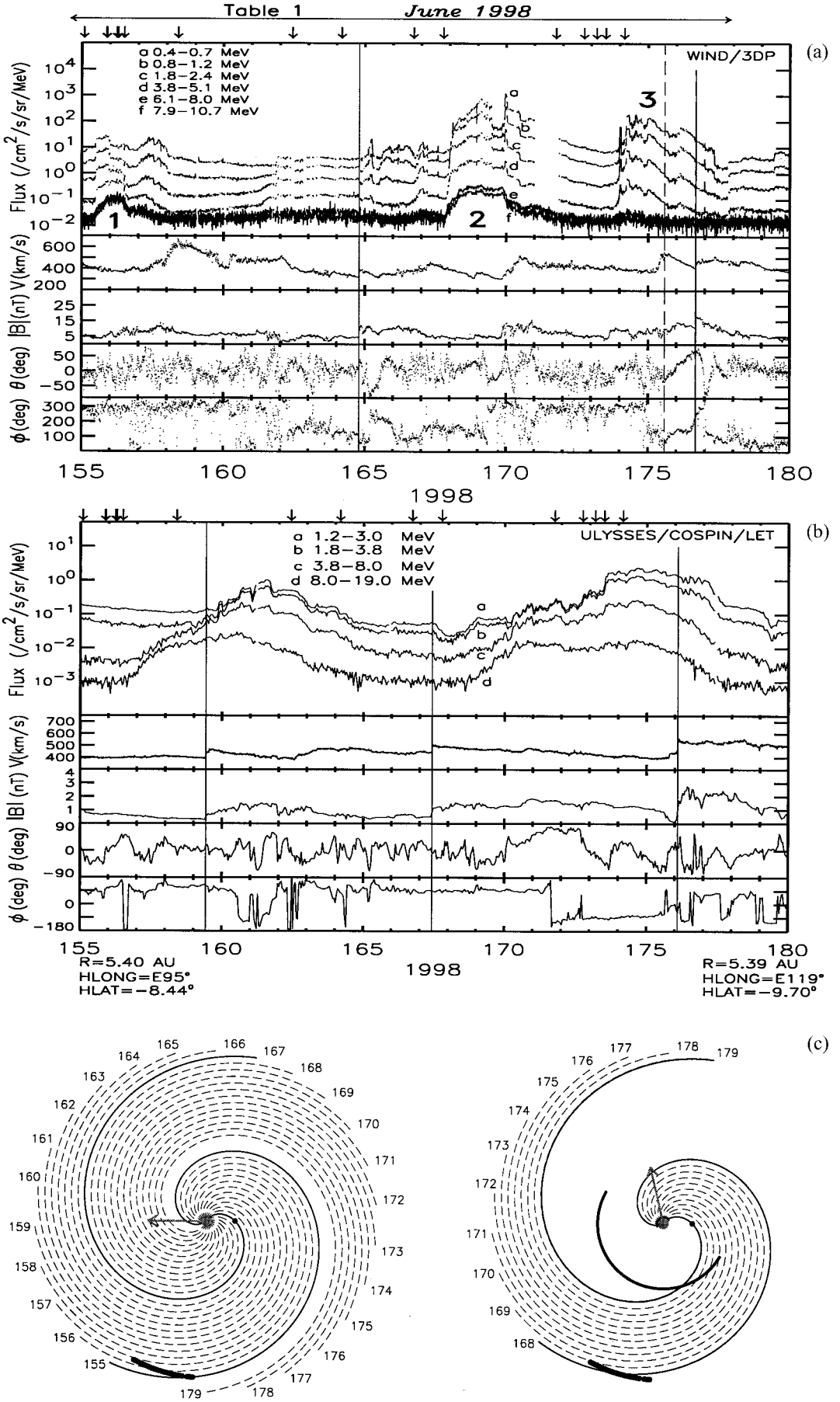

Figure 5. (a) Wind and (b) Ulysses observations for the June 1998 period; (c) spatial configuration of the ecliptic plane on (left) day 155 and (right) day 168 assuming a solar wind speed of 400 km s^{-1}. See text for details.

observations we cannot determine the possible solar origin of this cloud. The onset of this SEP event suggests that it occurred as a consequence of the FD at 173/1212 UT which was not efficient accelerating protons at energies above 5 MeV. However, possible contributions from previous and later solar events (as the west CME at 174/0359 UT) cannot be discarded.

3.3.2. Ulysses observations. During June 1998, Ulysses detected two extended proton flux enhancements separated by a period of flat flux profiles. Although the high intensity of the low-energy proton fluxes observed by Ulysses prior to the two proton events does not allow us to see their real onset (see Figure 1), there are features suggestive of velocity dispersion in both events, indicating a direct propagation of particles from their source to Ulysses. The first onset is also characterized by a strong antisunward flow of particles [*Dalla and Balogh*, 2000]. We suggest that the fast halo CME at 155/0204 UT, originated behind the west limb, together with the two backside events at the end of the same day, were most probably responsible for this first onset. These backside CMEs would have occurred from a region close to the root of the IMF connecting with Ulysses, and were able to accelerate energetic particles that were observed by Ulysses between days 156 and 164. The arrow in the left bottom panel of Figure 5 shows a possible direction of propagation for this backside CME. The second CME associated with the FDs on day 156 and other halo CMEs on days 156 and 158 (Table 1) might also contribute to inject energetic protons on to those field lines plotted as dashed lines in the left bottom panel of Figure 5 and that crossed the Ulysses spacecraft some days later.

The onset of the second SEP event at Ulysses occurs at the end of day 168. The high proton flux existing at that moment (Figure 1), together with the IMF orientation evolving from southern to northern, modifies the regular onset of this SEP event. Second-order anisotropies were observed from day 169 to 173, which represents a bidirectional flow of particles arriving at Ulysses [*Dalla and Balogh*, 2000]. We suggest that the rotational character of the IMF was due to a large magnetic structure which was filled with energetic particles. The source of particles was most probably related to the CME at 167/1827 UT which generated the SEP event number 2 at Wind. The arrow in Figure 5c (right) sketches the propagation direction of this CME. The shock driven by this CME injected protons on to those IMF lines connecting to Ulysses on days 169–173 days and that probably belonged to a magnetic structure whose origin we cannot determine.

At the end of day 173, IMF recovered the in-ecliptic orientation, and anisotropy recovered the antisunward character [*Dalla and Balogh*, 2000]. Energetic protons accelerated by the shock driven by the CME at 167/1827 UT were still arriving at Ulysses. Contribution from the solar events between days 171–174 together with the arrival at Ulysses of the interplanetary forward shock at 176/0220 UT cannot be discarded. The only possible association of this shock with a transient event occurring at the Sun is the CME on day 162 (Table 1) propagating away from the east limb of the Sun ($\langle v \rangle \simeq 684$ km s^{-1}); the front of this shock has been plotted in Figure 5c (right). The other two shocks observed by Ulysses at 159/1025 UT and 167/1029 UT (solid lines in Figure 5b) do not yield any contribution to the observed proton flux and their origin is not discussed here.

3.4. August 1998

The study of this period is specially complex because Ulysses was located in a diametrically opposed position with respect to Wind; reaching conjunction with the Sun on day 245. Therefore it is virtually impossible to associate the transient plasma signatures observed by Ulysses with the solar events observed near Earth. However, the nominal topology of the IMF (Figure 6, bottom) shows that Ulysses was magnetically connected to the west of the Sun, close to the connecting point of Wind. This fact helps us to relate the SEP events observed by Wind and Ulysses. Owing to the lack of LASCO data throughout this period, we use ground-based MLSO coronagraph observations.

3.4.1. Wind observations. Figure 6a shows Wind observations from day 228 to day 264. The sequence of eastern solar events from AR 8307 (from day 228 to 231; see Table 1) did not generate any special SEP event at Wind, mainly due to the poor magnetic connection between Wind and the source region of these CMEs. As this active region was approaching Central Meridian longitudes, the associated CMEs started having an effect on Wind particle observations. There was a first gradual increase of proton flux (for more than 3 days) characteristic of far eastern solar events [*Reames et al*., 1996], which we interpret as the arrival at Wind (by the corotation effect) of those IMF lines along which energetic particles coming from the eastern solar events generated by AR 8307 propagated. The arrival of a magnetic cloud at Wind between 232/~1000 UT and 233/~1900 UT did not have any influence on the proton fluxes at these enegies and its origin is not discussed here. The two solar events on days 234 and 235 from E51° and E33° respectively, contributed to the increase of the proton flux number 1 in Figure 6 (top). It is also possible that the shocks driven by the CMEs propagating away from the east limb of the Sun (from day 228 to 231) injected particles into their downstream regions contributing to this SEP event at Wind. A new SEP event (number 2) superimposed onto the decaying phase of the SEP event number 1. The origin of this new injection of particles has been associated with a flare from N35°E09° at 236/2212 UT [*Tylka et al*., 1999]. An interplanetary shock arrived at Wind at 238/0636 UT and produced an ESP event. The arrival of this shock suggests the existence of an Earth-directed CME propagating at an average transit speed of $\langle v \rangle \simeq 1283$ km s^{-1}. The lack of observation of this possible CME is not surprising since the field of view of MLSO is ±30° from the limb of the Sun.

The level of solar activity declined abruptly at the end of day 236 until day 242 when a new series of solar flares was observed but which did not produce any effect on particle flux at Wind, probably either because Wind was observing the decay phase of the event number 2 or because they were not efficient particle accelerators. A small SEP event was observed by Wind on day 249 (number 3 in Figure 6) and cannot be associated with any reported solar event seen from the Earth, and probably (by its West-type profile) was related to a backside west event; however, no coronal activity was seen by MLSO during their short daily observation time (see http://www.hao.ucar.edu/public/research/). Finally, another SEP onset was observed by Wind on day 252 (number 4 in Figure 6), which we attribute from its West-type signatures to the solar event associated with the flare at 252/0458 UT from S22°W65° (Table 1).

3.4.2. Ulysses observations. Figure 6 (middle) shows Ulysses proton observations for the period under study. Intervals

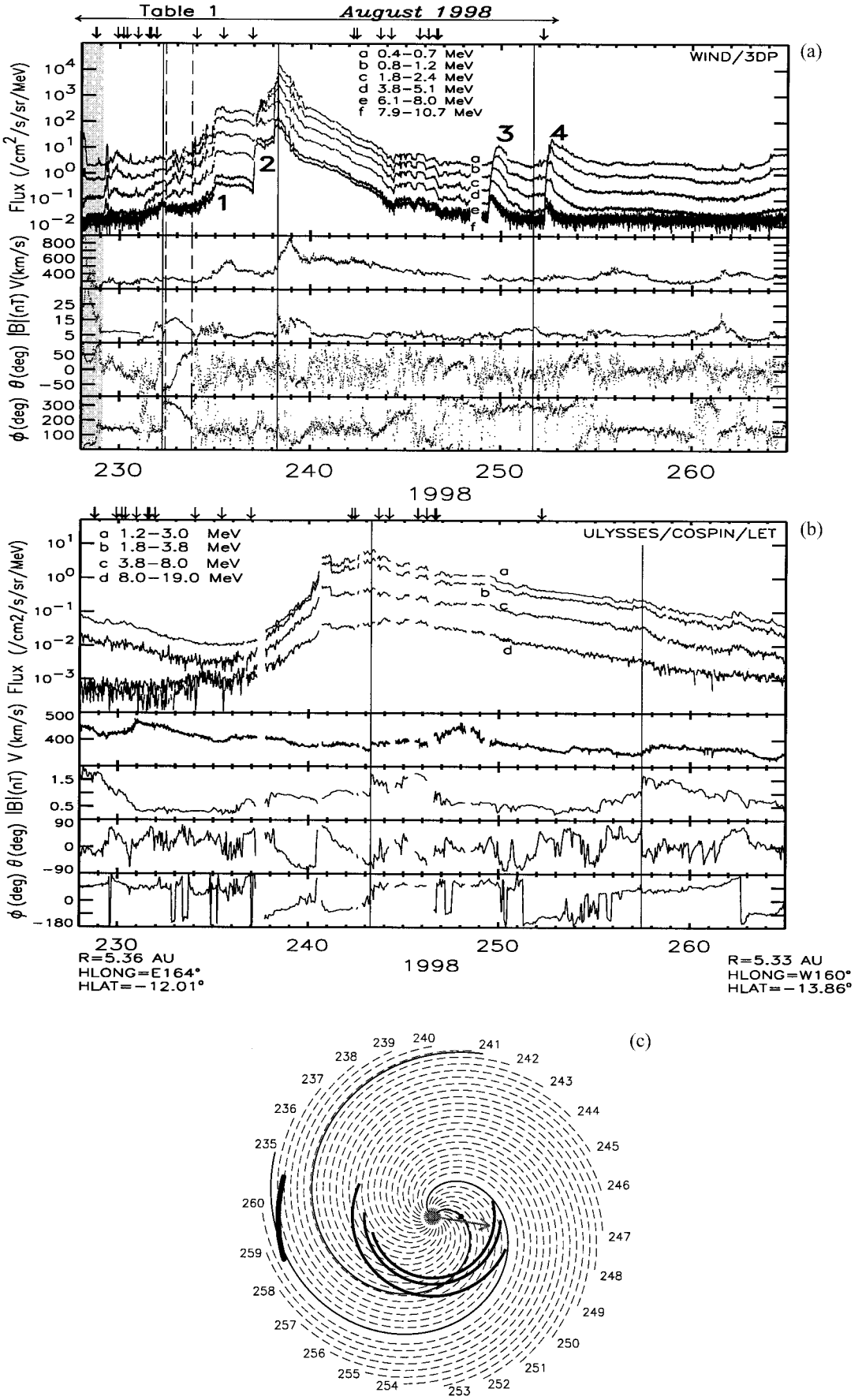

Figure 6. (a) Wind and (b) Ulysses observations for the August 1998 period. Shading bar in the top panel indicates the crossing of the Wind spacecraft through the Earth's magnetosphere. (c) Spatial configuration of the ecliptic plane on day 235 assuming a solar wind speed of 400 km s^{-1}. The arrow represents the propagation direction of the CME on day 236 causing the SEP event number 2 at Wind. See text for details.

of data gaps are due to the conjunction with the Sun which prevents a complete tracking of the spacecraft. Proton observations at Ulysses show a long-lasting particle event with a high particle intensity for more than 25 days. The onset of the particle flux enhancement was observed at the beginning of day 236 before the occurrence of the CME at 236/2212 UT which generated the SEP event number 2 at Wind. Ulysses was, in principle, connected to the west limb of the Sun (Figure 6c), where no flares and CMEs have been reported (Solar-Geophysical Data, no. 649, 1998). We suggest that the set of solar events from eastern longitudes generated by AR 8307 were responsible for the long-lasting particle event at Ulysses. The arrival of the particles did not occur immediately after the occurrence of the flares and CMEs. In fact, the lack of relativistic electrons (Figure 2) for this event suggests that there was not magnetic connection between the source region of these solar events and Ulysses. However, the shocks associated with the CMEs, probably occurring at the same time and from the same location of these flares, propagated away from the east limb of the Sun and accelerated protons that propagated along the field lines crossing Ulysses from day 236 onward.

Figure 6c sketches the heliospheric situation on day 235. Three shock fronts have been plotted in association with the CMEs observed by MLSO on days 228, 229, and 231 and propagating at 770, 800, and 1830 km s^{-1} respectively, which probably merged into one shock after traveling a certain distance through the interplanetary medium. The resulting shock was able to establish magnetic connection with the IMF lines connecting to Ulysses and generate the observed long-lasting particle event at this spacecraft. Later on, the magnetic connection between the shock and Ulysses was lost. However, a high proton intensity was observed by Ulysses for the rest of the period considered in Figure 6. We suggest that the shocks related to the solar events occurring from day 242 onward contributed to maintain the high proton intensity. Those CMEs propagating away from the west limb of the Sun injected particles directly to the field lines connecting to Ulysses, and to those field lines that (by the corotation effect) crossed Ulysses some days later. We cannot exclude other possibilities coming from backside events, for example, at the onset of the SEP event at Ulysses, there is a long-lasting rotation of the IMF followed by a forward shock at 243/0643 UT. This structure is probably associated with a transient event from the nonvisible part of the Sun, whose contribution to the Ulysses proton intensity and association with solar events cannot be determined. Anisotropy analyses show a large anti-sunward flow for the whole period, with the exception of a small bidirectional flow for days 239 and 240 due to the rotation of the IMF [*Dalla and Balogh*, 2000] which probably is due to the arrival of an ejecta associated with a backside event.

3.5. September–October 1998

Figure 7 shows Wind and Ulysses observations and their respective locations from day 269 to day 301. Ulysses was still in the part of the heliosphere located behind the Sun as seen from the Earth; therefore we cannot associate the transient plasma signatures observed by Ulysses with solar events observed near the Earth. For this period, LASCO data were only available on day 288 and from day 295 onward. For the rest of the period we use MLSO coronagraph observations.

3.5.1. Wind observations. Wind observed four particle flux enhancements numbered from 1 to 4 in Figure 7a. The first event was associated with the arrival of an interplanetary shock at 267/2318 UT followed 5.5 hours later by a magnetic cloud. The solar event associated with this SEP event was a solar flare at 266/0713 UT from N18°E09° [*Richardson and Cane*, 1999]. Kilometric type II radio emission was observed in association with this event which indicates the presence of a traveling interplanetary shock (M. Reiner, http://www-istp.gsfc.nasa.gov/istp/events/1998sept23/). Unfortunately, MLSO performed only 2 hours of observations on that day (from 1825 to 2043 UT) and no coronal activity was seen. The possible CME associated with the origin of this event would have been an Earth-directed CME able to produce the observation of an interplanetary shock and a magnetic cloud at Wind. The association between this solar event and the shock gives $\langle v \rangle \simeq 1037$ km s^{-1}. The arrival of the shock is characterized by an intense ESP event with high proton fluxes at all energy channels, suggesting a very efficient shock acceleration and trapping of particles around its front. The passage of the cloud is characterized by the typical drop of proton flux [*Cane et al.*, 1995], which later recovered the values that they would have if an exponential decay occurred after the shock passage.

An intense West-type SEP event (number 2 in Figure 7) was observed by Wind with an abrupt onset at 273/~1400 UT. *Dietrich and Lopate* [1999] and *von Rosenvinge et al.* [1999] relate the origin of this SEP event to the solar flares from S28°W35° at 273/1338 UT and N23°W81° at 273/1434. No coronal activity was seen by MLSO from 1710 to 2224 UT on the same day. An interplanetary shock was observed by Wind at 275/0705 UT, which we associate with the east flank of the shock driven by a CME coming from the western solar events on day 273 ($\langle v \rangle \simeq 1002$ km s^{-1}). From day 280 to day 288 proton fluxes at Wind remained at background levels even though two solar events occurred on day 280 (Table 1). MLSO observed a CME in progress on day 280 at 1747 UT which was propagating away from the east limb of the Sun but too faint to compute its speed. We associate this CME with the flare from E65° at 280/1712 UT. The poor magnetic connection between these two solar events and Wind is the most probable reason for the lack of particles at Wind.

A slow halo Earth-directed CME was detected at 288/1004 UT associated with a filament eruption from N19°E10° (BPR, no. 1207, 1998). At the time of this FD, a high-speed solar wind stream was crossing Wind, and probably prevented the arrival of the energetic particles accelerated during the FD. A sector boundary crossing Wind at the beginning of day 290 implied the magnetic connection of this spacecraft to a flux tube populated with energetic particles which constituted the SEP event number 3. Low-energy (<5 MeV) proton fluxes peaked with the arrival of an interplanetary shock at 291/1928 UT. The association between this shock and the halo CME gives $\langle v \rangle \simeq 510$ km s^{-1}. Unfortunately, between days 288 and 295, LASCO observations were unavailable and no other CME was observed within this period. About 6 hours after the passage of the shock at 291/1928 UT, signatures of ejecta have been detected in the solar wind parameters (T. Zurbruchen, private communication, 1999). The IMF increased up to 25 nT, with polar angles pointing to the south throughout day 292. The magnetic flux tube where Wind remained connected under this configuration was more populated with high-energy protons than with low-energy protons. We cannot explain the origin of this high-energy proton population observed together with this irregular IMF regime. We point out the possible contribution from the western solar flare at 291/0145 UT. Later on, after the passage of the ejecta through Wind, a new SEP event (number

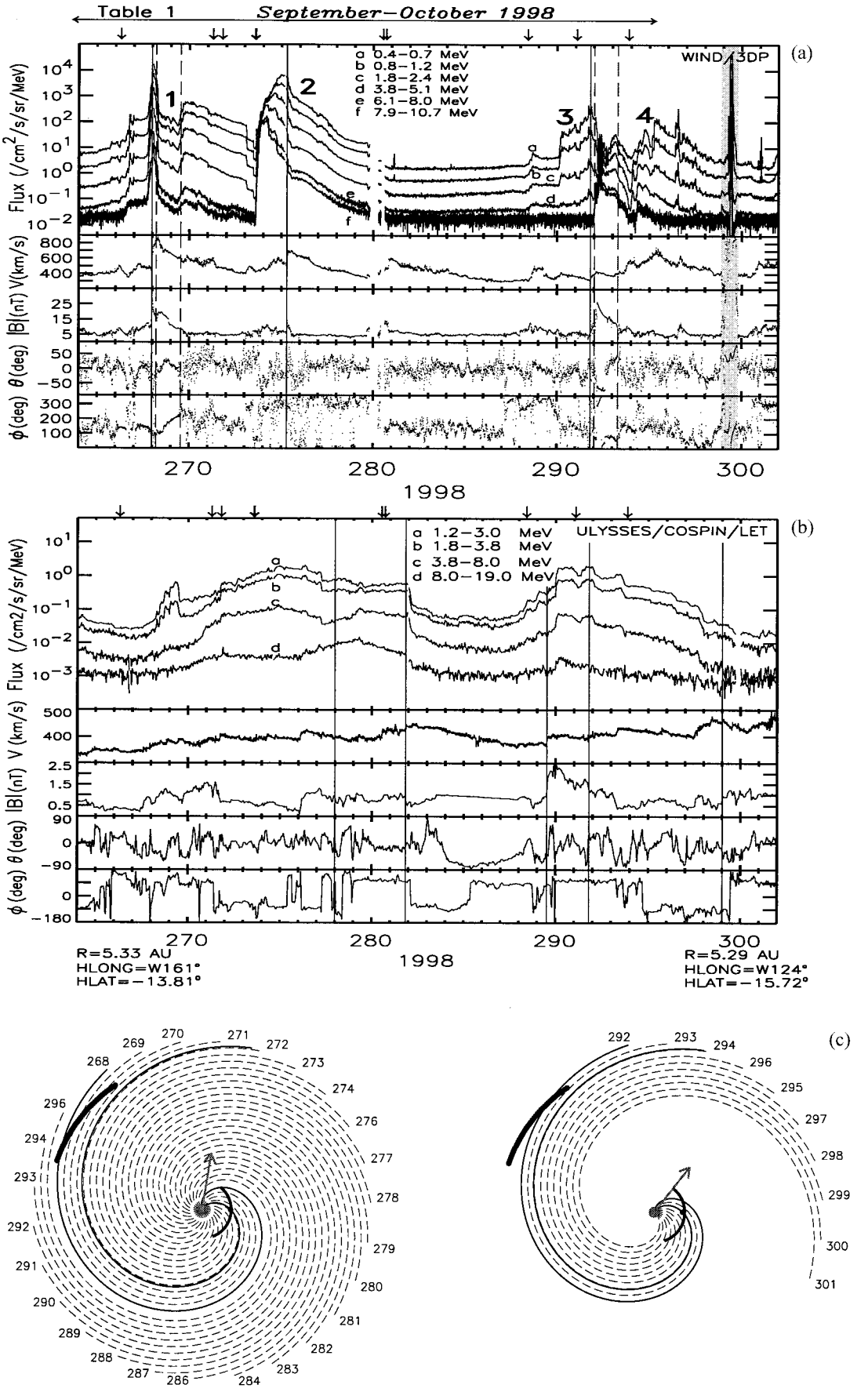

Figure 7. (a) Wind and (b) Ulysses observations for the September–October 1998 period. Shading bar in the top panel indicates the crossing of the Wind spacecraft through the Earth's magnetosphere. (c) Spatial configuration of the ecliptic plane on (left) day 268 and (right) day 292 assuming a solar wind speed of 400 km s^{-1}. See text for details.

4 in Figure 7) was observed. A long-duration X-ray flare occurred at 293/2103 UT without neither flare nor FD associated on the visible part of the Sun. The irregular shape of the proton flux profile at that time, together with the possible contribution from a high-speed solar wind stream on days 294–296, make the origin of this particle flux enhancement difficult to identify.

3.5.2. Ulysses observations. Ulysses particle observations show two main enhancements separated by a period of low proton intensities between days 282 and 289. The first particle onset was observed at low energies (<3.8 MeV) in association with a region of high IMF magnitude on day 267. The first high-energy (>8 MeV) protons did not arrive at Ulysses until day 268 with a gradual increase up to day 279. Anisotropy analyses show a strong particle streaming coming directly from the Sun for this period [*Dalla and Balogh*, 2000]. Figure 7c (left) sketches the heliospheric configuration on day 268; we have plotted a shock front associated with the CME which generated the SEP event number 1 at Wind when it arrived at this spacecraft. From this figure, we can see that the field lines observed by Ulysses between days 269–274 (dashed lines in Figure 7c (left)) were most probably populated by energetic particles accelerated by this fast shock. However, no direct magnetic connection between Ulysses and the site of the solar source of this CME was established, only when the associated CME-driven shock propagated well into the interplanetary medium, it was able to establish magnetic connection with Ulysses. In addition, Ulysses established first magnetic connection to the weak western flank of the shock, which in principle was only able to accelerate low-energy particles. The connection to the nose of the shock (more efficient accelerating high-energy protons as shown in Wind observations) was not established until the shock traveled a significant distance into interplanetary space (cobpoint concept [*Heras et al*., 1995]). That explains the delay between the solar event and the arrival of protons at Ulysses.

The arrow in the left bottom panel of Figure 7 identifies the solar site of the solar flare at 273/1434 UT (N23°W81°) where, according to the nominal IMF topology, Ulysses was directly connected. However, no relativistic electrons were observed at that time (Figure 2), either because the CME from the previous event distorted the IMF and Ulysses established magnetic connection with other solar regions not producing electrons, or because of the fact that this solar event was not efficient enough to accelerate electrons at these energies. In any case, the CME-driven shock associated with this western event contributed to extend the period of time when the Ulysses proton flux remained high.

The arrival at Ulysses of three sector boundaries on days 282, 285, and 288, together with out-of-ecliptic orientations of the IMF and depression of the proton flux, suggest the detection of a different particle population by the Ulysses spacecraft. We do not know whether, in the case that the IMF had remained with in-ecliptic orientations, the proton intensity would have maintained similar values as in the previous period. The fact is that in contrast to all other periods studied in this paper, anisotropy analyses show a sunward flow of particles [*Dalla and Balogh*, 2000], which suggests an origin for these protons different than a CME-driven shock propagating away from the Sun. The arrival of a forward-reverse shock pair at 289/1242 UT and 291/1924 UT resulted in a new increase of the proton intensities specially at energies below 8 MeV. The right bottom panel of Figure 7 sketches the heliospheric configuration on day 292 once the forward-reverse shocks (not plotted) crossed Ulysses. An interplanetary shock front associated with the CME at 288/1004 UT from N19°E10° (related to the SEP event number 3 at Wind) has been plotted assuming a radial expansion from E10° at a constant speed of 510 km s^{-1}. The arrow indicates the helilongitude of the solar event at 291/0145 UT from N16°W52° (Table 1). These two solar events probably contributed to inject accelerated particles on to those magnetic field lines connecting to Ulysses from day 292 onwards, extending the observation of high proton intensities and counteracting the sunward streaming of particles as anisotropy analyses indicate [*Dalla and Balogh*, 2000].

3.6. November 1998

3.6.1. Wind observations. Figure 8a shows Wind observations from day 309 to day 343. Part of data on days 329 to 333 was lost because on November 17, 1998 (day 321), Wind changed its orbit and the onboard telemetry antenna did not properly illuminate the tracking station. Existing data allow us to discern three main SEP events throughout November 1998 (numbered 1, 2, and 3 in Figure 8). The SEP event number 1, observed between days 310 and 315, was associated with a halo CME at 309/2044 UT in temporal association with a long-duration solar flare from N22°W18° (Table 1). Previously to this CME, two other halo CMEs occurred at 308/0418 UT and 309/0241 UT, presumably from the same active region AR 8375. Two interplanetary shocks were observed by Wind at 311/0800 UT and at 312/0440 UT. The first shock was probably associated with the CME at 308/0418 UT ($\langle v \rangle \simeq 549$ km s^{-1}), but it did not show a specific contribution to the proton flux which was already dominated by the protons accelerated by the second shock driven by the faster halo CME at 309/2044 UT. This shock arrived at Wind at 312/0440 UT ($\langle v \rangle \simeq 742$ km s^{-1}) and was followed by a magnetic cloud ~15 hours later. When this shock arrived at Wind, it still contributed to the proton flux at all energies which showed a local maximum at the time of its passage. On the next days (310–317) AR 8375 was specially active and produced numerous flares and CMEs from western longitudes (Table 1) which did not have a clear contribution to the proton flux at Wind, still on the decaying phase of the SEP event number 1.

The SEP event number 2 was observed by Wind in association with a solar event from the west limb of the Sun [*Dietrich and Lopate*, 1999; *von Rosenvinge et al*., 1999]. The crossing of Wind through the magnetosphere (gray shadow bars in Figure 8) prevents us from seeing the real onset of this SEP event. Unfortunately, LASCO observations were unavailable for this event and throughout MLSO's observing time (1702–2313 UT) no apparent coronal activity was seen. Two solar flares occurred at 318/0508 UT and 318/0519 UT from the west limb (Table 1). The West-type profile of this SEP event suggests that a western solar event contributed to the observed proton flux at Wind, but we cannot determine which one of these two solar events was the responsible for its origin. A new series of solar events occurred in the period between day 326 and 332 (Table 1). Data gaps from the Wind spacecraft and the crossing of this spacecraft through the Earth's magnetosphere (shaded bar in Figure 8) do not allow us to discern the effect of these solar events on the proton fluxes. In principle, for the particle onset observed on day 326 (number 3 in Figure 8), it seems that the efficiency of the solar events in accelerating particles was smaller than the two previous solar events on days 309 and 318.

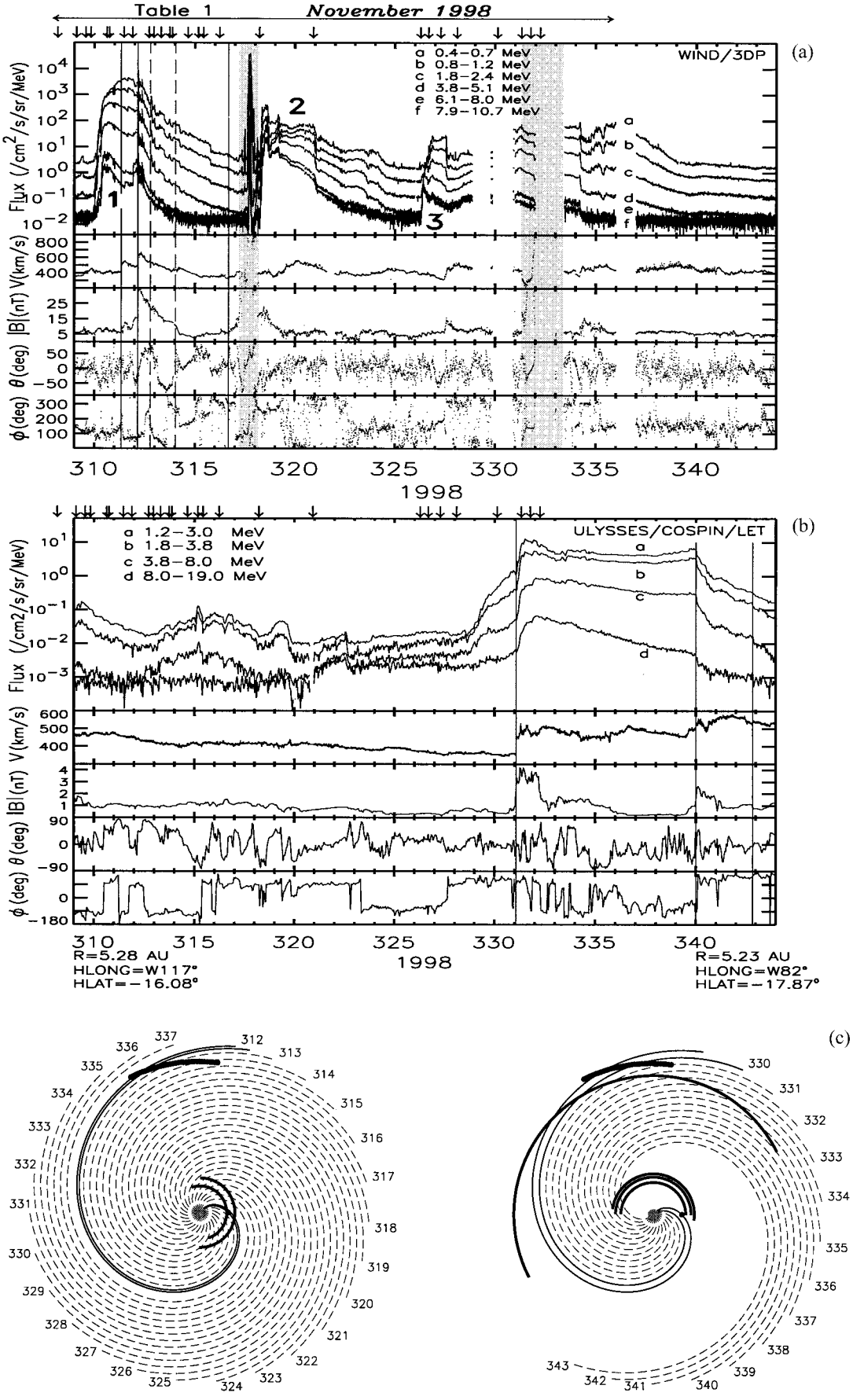

Figure 8. (a) Wind and (b) Ulysses observations for the November 1998 period. Shading bars in the top panel indicate the crossings of the Wind spacecraft through the Earth's magnetosphere. (c) Spatial configuration of the ecliptic plane on (left) day 312 and (right) day 330 assuming a solar wind speed of 400 km s^{-1}. See text for details.

3.6.2. Ulysses observations. The nominal magnetic field topology depicted in the bottom panels of Figure 8 shows that Ulysses and Wind were connected to close-by field lines; consequently, those SEP events observed by Wind, after propagation effects, have to be observed later by Ulysses. There is a first small SEP event at Ulysses observed only at low energies (<8 MeV) between days 312 and 317 and with a strong antisunward particle streaming [*Dalla and Balogh*, 2000]. The high proton intensity observed by Ulysses previously to the onset of this proton flux enhancement (see Figure 1a) does not allow us to see the arrival of the first particles associated with this event. We associate its origin with the CME at 309/2044 UT whose shock propagated directly to Wind producing the SEP event number 1 at this spacecraft. Figure 8c (left) sketches the heliospheric configuration on day 312 with two interplanetary shocks associated with the CMEs at 308/0418 UT and 309/2044 UT propagating at 549 and 742 km s^{-1} respectively. When these interplanetary shocks started propagating from the Sun, they established magnetic connection with Ulysses; after some propagation of these shocks through the interplanetary medium, the magnetic connection between the shocks and Ulysses was lost, and they did not contribute any more to the proton flux at Ulysses, explaining in this way the short time duration of this SEP event at Ulysses and its low intensity.

The solar event associated with the SEP event number 2 at Wind occurred from western longitudes (Table 1) and, in principle, close to the foot of the IMF line connecting to Ulysses. The increase of relativistic electron intensity at that time (Figure 2) suggests that direct magnetic connection between Ulysses and the solar events existed. Ulysses proton flux increased at the beginning of day 320 with features suggestive of velocity dispersion and with antisunward flow of particles [*Dalla and Balogh*, 2000]. The increase of the proton flux became more pronounced two days before the arrival of a strong shock at 331/0146 UT. After the shock passage, the proton flux kept increasing until a maximum of proton intensity at the end of day 331. The low-energy proton flux remained at an approximate constant value for more than 8 days until the arrival of a second strong forward shock at 339/2353 UT when it showed a local maximum around the shock passage and a subsequent decay. The high-energy proton flux was already decaying before the arrival of the second shock.

We suggest the following scenario to explain these observations. The solar source of the CME at 318/0508 UT was well aligned to generate a shock observed by Ulysses. The association of this CME with the shock observed by Ulysses at 331/0146 UT gives an average transit shock speed $\langle v \rangle \simeq 708$ km s^{-1}. Figure 8c (right) shows the ecliptic-plane configuration on day 330; a wide shock propagating from western longitudes and almost arriving at Ulysses has been plotted as a representation of the shock observed by Ulysses at 331/0146 UT. Before the arrival of this shock at Ulysses, the sequence of solar events from day 326 to 330 took place (Table 1). Protons accelerated in these events filled the downstream region of this shock which was acting as a magnetic barrier for those particles. These particles bounced back and forward between the first shock and a second shock, which may be associated either with a compression region of a high-speed ($\sim$600 km s^{-1}) solar wind stream observed together with the arrival of a reverse shock at 342/2016 UT or with the western solar events from day 326 to 330. According to the solar longitude of these latter solar events a possible shock driven by the associated CMEs was also able to reach Ulysses. The shock fronts associated with each one of these solar events have been plotted in the right bottom panel of Figure 8 but, probably, after some interplanetary propagation, these shocks merged into one. The association between the second shock observed by Ulysses at 339/2353 UT and the fast halo CME at 328/0230 UT (originated from a backside southwest event (ftp://lasco6.nascom.nasa.gov/pub/lasco/status/) gives $\langle v \rangle \simeq 764$ km s^{-1}. Therefore two shocks were propagating at similar speeds with an energetic particle population bouncing between them. In the case of a high-speed stream, however, those shocks associated with the solar events on days 326–330 were not able to reach Ulysses. Energetic particles between the forward shocks at 331/0146 and 339/2353 UT were not only trapped between the two shocks but also underwent shock-acceleration processes resulting in the constant flux observed at low-energies. We point out also that between the shocks, there was a region of very low IMF magnitude between days 336 and 338 which may be a good region to keep those particles mirroring between two boundaries of higher IMF magnitude. Figure 8c (right) we have maintained the spiral structure for the IMF lines for consistency with other figures. However, the conceptual image for the IMF in the downstream region of interplanetary shocks [*Lario et al*., 1999a] shows a distorted structure for the magnetic field lines which may be more radial and suggesting a real magnetic connection between the two shocks allowing the particles to bounce between them. Anisotropy studies show a remarkable phase of constant zero anisotropy between day 335 and 339 which supports our suggested scenario [*Dalla and Balogh*, 2000].

4. Discussion

We have presented here a complete study of the largest SEP events observed by the Wind and Ulysses spacecraft from October 1997 to the end of December 1998. The events at both spacecraft are associated with periods of intense solar activity in the rising phase of the solar cycle 23. The proton flux profiles of these SEP events look different at 1 and $\sim$5 AU. Whereas at 1 AU a number of SEP events can be distinguished and associated with individual CMEs within a short period of time, at 5 AU the events have longer time durations, smooth flux profiles, and show less details than at 1 AU. This pattern is representative of all the selected periods (see Figures 3–8); the most significant case is in April–May 1998 when Wind detected six separated SEP events from day 110 to 135, but Ulysses only saw a single long-lasting SEP event. The two main factors responsible for these observations are (1) the larger number of interplanetary processes acting upon the particles throughout their journey from the Sun to Ulysses and (2) the different number of CMEs occurring throughout the development of an SEP at Wind and at Ulysses.

In order to illustrate the effects of particle propagation in broadening and extending the intensity time profiles at Ulysses we have simulated the transport of particles along a given magnetic field line. The assumptions adopted in these simulations are described in the appendix. We have considered two simple cases illustrative of the physical processes occurring during the development of the particle flux enhancements observed at 1 and at 5 AU. The first case considers an initial anisotropic distribution close to the Sun. The second case considers the same initial distribution but an additional injection of an identical distribution 5 hours after the initiation of the simulation. Figure 9 shows the intensity of particles ob-

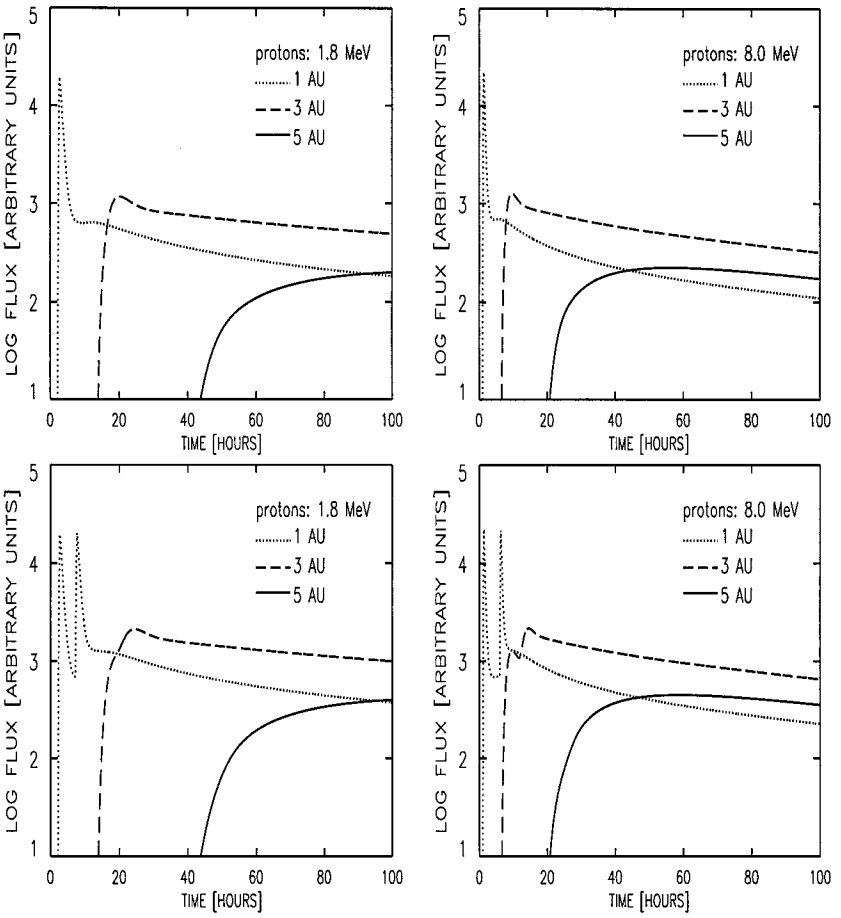

Figure 9. Simulated evolution of the (left) 1.8 MeV and (right) 8.0 MeV proton flux for three observers located at heliocentric distances of 1, 3, and 5 AU assuming (top) an initial injection close to the Sun or (bottom) two injections separated 5 hours.

served at three heliocentric radial distances of 1, 3, and 5 AU, which correspond to three observers located on the same Archimedian spiral field line at 1.17, 5.93, and 14.74 AU from the Sun, respectively. The two top panels show the case with only one impulsive injection from a point close to the Sun. The basic features of a rapid rise and slow decay characteristic of the SEP events observed at 1 AU in the absence of traveling shocks are reproduced for the first two observers. However, the intensity of the peak decreases as we move to observers more distant from the Sun, mainly due to the continuous leakage of particles through the outer boundary of the simulation domain and the effects of pitch angle scattering [*Lario*, 1997]. The initial coherent and anisotropic pulse injected close to the Sun becomes spread into a broad range of pitch angle values as it moves away from the Sun, resulting in a population of particles moving in different directions along the field line. By giving more time for propagation effects to act upon the particle distribution (that means observers more distant from the Sun or particles of lower energy) the resulting proton flux profiles broaden and the observed period of high intensities lasts for a longer time. The same effect is responsible for the observation of two different peaks at 1 AU (due to two separate impulsive injections from the Sun) but only a smoothed down flux profile at 5 AU (Figure 9, bottom). Continuous injection of particles from traveling interplanetary shocks [*Lario et al*., 1998b], smaller mean free paths or the inclusion of adiabatic deceleration effects [*Lario*, 1997] will produce the general apparence of long-lasting periods of time with high proton intensities.

The occurrence of multiple CMEs during the time intervals analyzed in section 3 (Figures 3–8) modifies also the conditions under which the SEP events developed at 1 and at ~5 AU. As CMEs propagate through the interplanetary medium, they strongly distort the IMF and profoundly affect energetic particle propagation [*Lario et al*., 1999a]. The superposition of several such disturbances in the outer heliosphere can produce large-scale magnetic structures that impede the free streaming of energetic particles injected from successive solar events [*Roelof et al*., 1992]. That is the case for those particles injected by the CME at 310/1210 UT in 1997 and observed inside the magnetic cloud arriving at Ulysses at 317/0830 UT, and for those particles contained between the two shocks arriving at Ulysses at 331/0146 UT and 339/2353 UT in 1998.

The rapid arrival and passage of CMEs through the Wind location avoids the formation of these structures and the trapping of particles. On the contrary, the SEP events observed at 1 AU are in most of the cases associated with single and isolated CMEs. Our selection of SEP events is based on those periods with a high proton intensity, and therefore, it leads to a bias of events generated by CMEs from the west limb of the Sun or from near Central Meridian [*Cane et al*., 1988]. For those events, Wind establishes magnetic connection to the

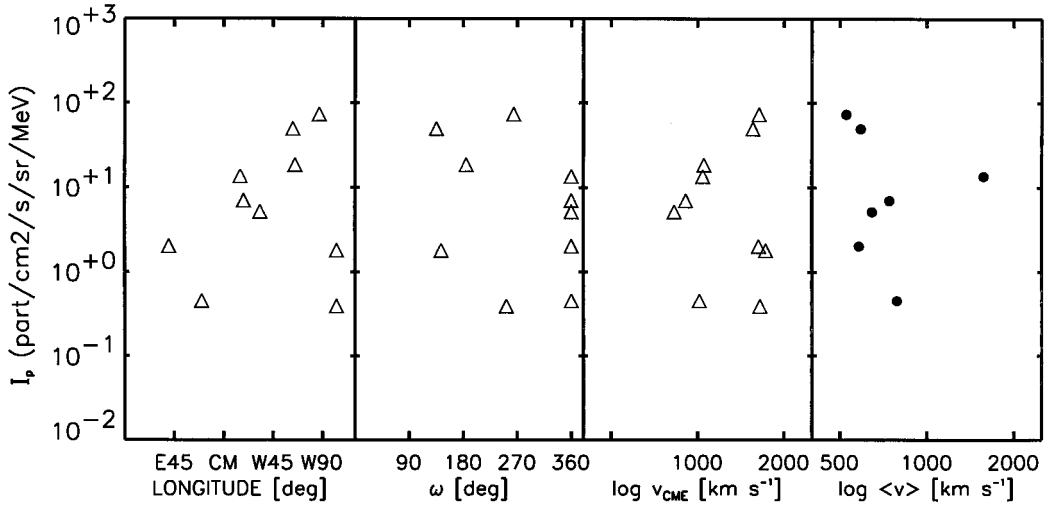

Figure 10. Relationship between the peak 6.1–8.0 MeV proton intensity I_p observed by Wind at 1 AU, and the longitude, angular width, and speed of the CMEs for the selected SEP events (triangles) and the transit shock speed $\langle v \rangle$ (black dots) for those SEP events observed in association with transient interplanetary shocks.

nose of CME-driven shocks (in principle, the region most efficient accelerating particles) when they start propagating from the Sun or when they arrive at 1 AU. The association between SEP events at 1 AU and specific CMEs (eleventh column in Table 1) offers us the opportunity to compare the intensities of the SEP events with the parameters of the CMEs. We have selected those events (indicated by a triangle in the eleventh column of Table 1) whose association with a single and isolated CME is unquestionable and whose 6.1–8.0 MeV flux profiles reach a maximum without the contribution of any other SEP event. Figure 10 shows the correlations between the peak 6.1–8.0 MeV proton intensity I_p, and the longitude, angular width, and speed of the CMEs. Note that our sample of events is restricted to CMEs with $v_{\mathrm{CME}} > 800$ km s^{-1} and five of them are halo CMEs ($\omega = 360°$). The four particle events with lowest I_p values correspond to those events generated from eastern longitudes (SEP events number 3 and 4 in the April–May 1998 period) and to those events generated from behind the west limb of the Sun (SEP events number 7 in April–May 1998 and number 2 in June 1998; the origin of the SEP event number 2 in the April–May 1998 period is considered W87° in Figure 10). We see that, at these energies, the most intense SEP events seem to be associated with western and fast CMEs; however, no obvious correlation is found for ω. These results corroborate the results found by *Kahler et al.* [1999]. On the other hand, Wind also observed the associated transient shocks in seven of these SEP events (indicated by a black dot in the eleventh column of Table 1). For those events we have also compared the shock transit speed $\langle v \rangle$ with I_p (Figure 10, right), but no obvious correlation was found. We should note that I_p was not always found at the time of the shock arrival at Wind, mainly due to the West-type profile of some of these events. These results show that other factors different than $\langle v \rangle$ or ω may have a stronger influence on the production of SEP events; they are probably the seed particle population available to be accelerated, or the characteristics and evolution of the shocks and their connection to the spacecraft as they propagate from the Sun to the observer [*Lario et al.*, 1998b; *Kahler et al.*, 1999]. Unfortunately, a similar analysis for the SEP events observed by Ulysses cannot be done due to the occurrence of several CMEs throughout the development of a single SEP event at 5 AU, and the impossibility of identifying unequivocally the source of particles in a given solar event.

5. Conclusions

In summary, our study of the energetic proton observations from the Wind and Ulysses spacecraft in the rising phase of solar cycle 23 allows us to conclude that:

1. Periods of intense solar activity produce SEP events at Wind and Ulysses even when their longitudinal and radial separation is large. The development of SEP events at both spacecraft is due to CME-driven shocks able to accelerate and to inject particles into a large fraction of the heliosphere as they move through interplanetary space.

2. Separated SEP events at 1 AU become merged at 5 AU, suggesting that interplanetary processes acting upon the particles, due to traveling magnetic field structures (shocks, clouds, etc.) and to particle transport effects, are responsible for broadening and smoothening the flux profiles at 5 AU. Our simulation, including only the particle transport effects, shows that the flux profiles broaden and smoothen with increasing distance from the Sun.

3. In contrast to 1 AU, the classification of SEP event profiles as West-, East-, or Central Meridian-type is not useful in the outer heliosphere. Under ideal conditions, i.e., a single and isolated CME throughout the development of the SEP at Ulysses, a CME-driven shock efficient enough to accelerate particles throughout its journey from the Sun to ~5 AU and throughout its front of a given width, and a perfect delimited IMF connection between the spacecraft and the shock; it would be possible to describe a similar classification for the SEP events depending on where the CME develops with respect to the root of the IMF line connecting Ulysses and whether the CME-driven shock will intercept (where and when) this IMF line. However, observations throughout 1997 and 1998 show that this is not the case. The topology of the IMF, the occurrence of several CMEs, as well as the set of traveling CME-driven shocks and magnetic structures are the

main factors responsible for this lack of longitudinal dependence of the SEP events at Ulysses.

4. In contrast to 1 AU the observation of SEP events at Ulysses does not require the arrival of interplanetary shocks at the spacecraft or the magnetic connection when these shocks start propagating from the Sun. The events of August 1998, for example, show that a set of CMEs (from day 228 to 236) started propagating from regions quite distant to the root of the IMF line connecting to Ulysses. At some stage of their expansion, well into interplanetary space (as indicated in Figure 6c), those shocks established magnetic connection with Ulysses and produced SEP events at this spacecraft. Later on, the magnetic connection between Ulysses and these shocks was lost and they did not contribute any more to the proton flux observed by Ulysses. Moreover, the successive connection of Ulysses with those field lines along which energetic particles from previous solar events propagate, extends the duration of SEP events in the outer heliosphere and complicates the identification of the source of the particles arriving at Ulysses.

Appendix: Energetic Particle Transport

The propagation of particles along a given magnetic field line is described by the focusing-diffusion transport equation developed by *Roelof* [1969]:

$$\frac{\partial F(t,\,\mu,\,z)}{\partial t} + \frac{\partial}{\partial z}\left(v\mu F(t,\,\mu,\,z)\right) + \frac{\partial}{\partial \mu}\left[\frac{1-\mu^2}{2L(z)}\,vF(t,\,\mu,\,z)\right] - \frac{\partial}{\partial \mu}\left[\varphi(\mu)\,\frac{\partial F(t,\,\mu,\,z)}{\partial \mu}\right] = 0, \tag{A1}$$

where $F(t,\,\mu,\,z) = dN/d\mu dz$ is the density of particles, t is the time, μ is the pitch angle cosine, z is the distance along the field line, v is the particle velocity, L is the focusing length $L = -B/(\partial B/\partial z)$, and B is the mean magnetic field computed assuming an Archimedian spiral magnetic field with a solar wind speed of 400 km s^{-1}. The pitch angle scattering coefficient, $\varphi(\mu)$ is expressed according to the quasi-linear theory [*Jokipii*, 1971] as $\varphi(\mu) = A|\mu|^{q-1}(1-\mu^2)$ with $A = 3v/[2\lambda_{//}(4-q)(2-q)]$, where $\lambda_{//}$ is the mean free path of the particles parallel to the magnetic field and q is the spectral index of the power spectrum of the magnetic field. This expression has been usually adopted as a convenient and widely used parametrization to describe the effects of the magnetic field fluctuations on particle transport. In our simulation, we consider $\lambda_{//} = 2$ AU and $q = 1.5$, which are in the range of values inferred by *Bieber et al.* [1986] for interplanetary scattering inside of 1 AU. We assume that these conditions are still valid to describe the transport out to 5 AU. Two absorbing boundaries have been considered at the inner z grid point ($z = 0.05$ AU from the Sun along the flux tube) and at the outer z grid point ($z = 17$ AU). Particles arriving at the inner boundary with $\mu < 0$ or arriving at the outer boundary with $\mu > 0$ are allowed to flow out and they are no longer considered in the computation. The numerical scheme to solve (A1) is explained by *Lario* [1997].

Acknowledgments. We acknowledge the use of the Ulysses Data System (UDS). We appreciate J. T. Burkepile and MLSO/MK3 team for the use of their CME lists. We acknowledge the use of data from the Ulysses/COSPIN/KET experiment and from the Wind MFI experiment (P. I.: R. P. Lepping). D. L. and M. M. were supported by ESA Research Fellowships.

Janet G. Luhmann thanks Steven W. Kahler and Donald V. Reames for their assistance in evaluating this paper.

References

Balogh, A., T. J. Beeck, R. J. Forsyth, P. C. Hedgecock, R. J. Marquedant, E. J. Smith, D. J. Southwood, and B. T. Tsurutani, The magnetic field investigation on the Ulysses mission: Instrumentation and preliminary results, *Astron. Astrophys. Suppl. Ser.*, *92*, 221, 1992.

Bame, S. J., D. J. McComas, B. L. Barraclough, J. L. Phillips, K. J. Sofaly, J. C. Chavez, B. E. Goldstein, and R. K. Sakurai, The Ulysses solar wind plasma experiment, *Astron. Astrophys. Suppl. Ser.*, *92*, 237, 1992.

Bieber, J. W., P. A. Evenson, and M. A. Pomerantz, Focusing anisotropy of solar cosmic rays, *J. Geophys. Res.*, *91*, 8713, 1986.

Brueckner, G. E., et al., The large angle spectroscopic coronagraph (LASCO), *Sol. Phys.*, *162*, 357, 1995.

Cane, H. V., R. E. McGuire, and T. T. von Rosenvinge, Two classes of solar energetic particle events associated with impulsive and long-duration soft X-ray flares, *Astrophys. J.*, *301*, 448, 1986.

Cane, H. V., N. R. Sheeley Jr., and R. A. Howard, Energetic interplanetary shocks, radio emission, and coronal mass ejections, *J. Geophys. Res.*, *92*, 9869, 1987.

Cane, H. V., D. V. Reames, and T. T. von Rosenvinge, The role of interplanetary shocks in the longitude distribution of solar energetic particles, *J. Geophys. Res.*, *93*, 9555, 1988.

Cane, H. V., I. G. Richardson, and G. Wibberenz, The response of energetic particles to the presence of ejecta material, *Conf. Pap. Int. Cosmic Ray Conf. 24th*, *4*, 377, 1995.

Cliver, E. W., S. W. Kahler, D. F. Neidig, H. V. Cane, I. G. Richardson, M.-B. Kallenrode, and G. Wibberenz, Extreme "propagation" of solar energetic particles, *Conf. Pap. Int. Cosmic Ray Conf. 24th*, *4*, 257, 1995.

Dalla, S., and A. Balogh, Recurrence in MeV proton fluxes and anisotropies at 5 AU from the Sun, *Geophys. Res. Lett.*, *27*, 153, 2000.

Dietrich, W., and C. Lopate, Measurements of iron rich SEP events using the University of Chicago IMP-8 instrument, *Conf. Pap. Int. Cosmic Ray Conf. 24th*, *6*, 71, 1999.

Fisher, R. R., R. H. Lee, R. M. MacQueen, and A. I. Poland, New Mauna Loa coronagraph systems, *Appl. Opt.*, *20*, 1094, 1981.

Harrison, R. A., The nature of solar flares associated with coronal mass ejections, *Astron. Astrophys.*, *304*, 585, 1995.

Heras, A. M., B. Sanahuja, Z. K. Smith, T. Detman, and M. Dryer, The influence of the large-scale interplanetary shock structure on a low-energy particle event, *Astrophys. J.*, *391*, 359, 1992.

Heras, A. M., B. Sanahuja, D. Lario, Z. K. Smith, T. Detman, and M. Dryer, Three low-energy particle events: Modeling the influence of the parent interplanetary shock, *Astrophys. J.*, *445*, 497, 1995.

Jokipii, J. R., Propagation of cosmic rays in the solar wind, *Rev. Geophys.*, *9*, 27, 1971.

Kahler, S. W., Injection profiles of solar energetic particles as functions of coronal mass ejection heights, *Astrophys. J.*, *428*, 837, 1994.

Kahler, S. W., J. T. Burkepile, and D. V. Reames, Coronal/interplanetary factors contributing to the intensities of $E > 20$ MeV gradual solar energetic particle events, *Conf. Ray Int. Cosmic Ray Conf. 26th*, *6*, 248, 1999.

Kallenrode, M.-B., E. W. Cliver, and G. Wibberenz, Composition and azimuthal spread of solar energetic particles from impulsive and gradual flares, *Astrophys. J.*, *391*, 370, 1992.

Kallenrode, M.-B., G. Wibberenz, H. Kunow, R. Müller-Mellin, V. Stolpovskii, and N. Kontor, Multi-spacecraft observations of particle events and interplanetary shocks during November/December 1982, *Sol. Phys.*, *147*, 377, 1993.

Lario, D., Propagation of low-energy particles through the interplanetary medium: Modeling their injection from interplanetary shocks, Ph.D. thesis, 294 pp., Univ. Barcelona, Barcelona, Spain, July 1997.

Lario, D., R. G. Marsden, T. R. Sanderson, M. Maksimovic, A. Balogh, R. J. Forsyth, R. P. Lin, and J. T. Gosling, Ulysses and WIND particle observations of the November 1997 solar events, *Geophys. Res. Lett.*, *25*, 3469, 1998a.

Lario, D., B. Sanahuja, and A. M. Heras, Energetic particle events: Efficiency of interplanetary shocks as 50 keV $< E <$ 100 MeV proton accelerators, *Astrophys. J.*, *509*, 415, 1998b.

Lario, D., M. Vandas, and B. Sanahuja, Energetic particle propagation in the downstream region of transient interplanetary shocks, in *Proceedings of the Ninth International Solar Wind Conference*, *AIP Conf. Proc. 471*, edited by S. R. Habbal, R. Esser, J. V. Hollweg, and P. A. Isenberg, p. 741, Woodbury, N. Y., 1999a.

Lario, D., R. G. Marsden, T. R. Sanderson, M. Maksimovic, A. Balogh, R. J. Forsyth, S. Dalla, and R. P. Lin, Solar energetic particle events in the rising phase of solar cycle 23: Observations at 1 and 5 AU, *Conf. Pap. Int. Cosmic Ray Conf. 26th*, *6*, 540, 1999b.

Lario, D., R. G. Marsden, T. R. Sanderson, M. Maksimovic, B. Sanahuja, A. Balogh, R. J. Forsyth, R. P. Lin, and J. T. Gosling, Energetic proton observations at 1 and 5 AU, I, January–September 1997, *J. Geophys. Res*., this issue.

Lee, M. A., Particle acceleration and transport at CME-driven shocks, in *Coronal Mass Ejections*, *Geophys. Monogr. Ser*., vol. 99, edited by N. Crooker, J. A. Joselyn, and J. Feynman, p. 227, AGU, Washington, D. C., 1997.

Lepping, R. P., et al., The WIND magnetic field investigation, *Space Sci. Rev*., *71*, 207, 1995.

Lin, R. P., et al., A three-dimensional plasma and energetic particle investigation for the WIND spacecraft, *Space Sci. Rev*., *71*, 125, 1995.

Mäkelä, P., M. Teittinen, and J. Torsti, Solar particle eruptions observed by SOHO/ERNE in November 1997, *Conf. Pap. Int. Cosmic Ray Conf. 26th*, *123*, 1999.

Marsden, R. G., D. Lario, T. R. Sanderson, M. Maksimovic, A. Balogh, S. Dalla, and R. J. Forsyth, On the energetic particle fluxes at 5 AU associated with the April/May 1998 solar activity: Ulysses observations, in *Proceedings of the Ninth International Solar Wind Conference*, *AIP Conf. Proc. 471*, p. 609, edited by S. R. Habbal, R. Esser, J. V. Hollweg, and P. A. Isenberg, Woodbury, N. Y., 1999.

Mason, G. M., et al., Particle acceleration and sources in the November 1997 solar energetic particle events, *Geophys. Res. Lett*., *26*, 141, 1999.

McKenna-Lawlor, S. M. P., K. Kecskeméty, V. Bothmer, J. Rodríguez-Pacheco, G. Facskó, and C. St. Cyr, Solar Energetic particle events recorded aboard SOHO on December 24, 1996 and on May 6, 1998, *Conf. Pap. Int. Cosmic Ray Conf. 26th*, *6*, 423, 1999.

Reames, D. V., Particle acceleration at the Sun and in the heliosphere, *Space Sci. Rev*., *90*, 413, 1999.

Reames, D. V., L. M. Barbier, and C. K. Ng, The spatial distribution of particles accelerated by coronal mass ejection-driven shocks, *Astrophys. J*., *466*, 473, 1996.

Reames, D. V., S. W. Kahler, and C. K. Ng, Spatial and temporal invariance in the spectra of energetic particles in gradual solar events, *Astrophys. J*., *491*, 414, 1997.

Reiner, M. J., M. L. Kaiser, J. Fainberg, and R. G. Stone, A new method for studying remote type II radio emissions from coronal mass ejection-driven shocks, *J. Geophys. Res*., *103*, 29,651, 1998.

Richardson, I. G., and H. V. Cane, Bidirectional ~1 MeV ion flows observed by IMP8 over two solar cycles, *Conf. Pap. Int. Cosmic Ray Conf. 26th*, *6*, 436, 1999.

Roelof, E. C., Propagation of solar cosmic rays in the interplanetary magnetic field, in *Lectures in High Energy Astrophysics*, edited by H. Ögelman and J. R. Wayland, *NASA Spec. Publ*., *SP-199*, 111, 1969.

Roelof, E. C., R. E. Gold, G. M. Simnett, S. J. Tappin, T. P. Armstrong, and L. J. Lanzerotti, Low energy solar electrons and ions observed at Ulysses February–April 1991: The inner heliosphere as a particle reservoir, *Geophys. Res. Lett*., *19*, 1243, 1992.

Sanderson, T. R., D. Lario, M. Maksimovic, R. G. Marsden, C. Tranquille, A. Balogh, R. J. Forsyth, and B. E. Goldstein, Current sheet control of recurrent particle increases at 4–5 AU, *Geophys. Res. Lett*., *26*, 1785, 1999.

Simpson, J. A., et al., The Ulysses cosmic ray and solar particle investigation, *Astron. Astrophys. Suppl. Ser*., *92*, 365, 1992.

Timofeev, V. E., and S. A. Starodubtsev, Solar energetic particle events at the rise phase of the 23rd solar activity cycle registered aboard the spacecraft Interball-2, *Conf. Pap. Int. Cosmic Ray Conf. 26th*, *6*, 200, 1999.

Torsti, J., and T. Sahla, Development of directional flux anisotropy during the solar event on June 16, 1998, *Conf. Pap. Int. Cosmic Ray Conf. 26th*, *6*, 336, 1999.

Tylka, A. J., D. V. Reames, and C. K. Ng, Observations of systematic temporal evolution in elemental composition during gradual solar energetic particle events, *Geophys. Res. Lett*., *26*, 2141, 1999.

von Rosenvinge, T. T., et al., Time variations of solar energetic particle abundances observed by the ACE spacecraft, *Conf. Pap. Int. Cosmic Ray Conf. 26th*, *6*, 131, 1999.

A. Balogh and R. J. Forsyth, The Blackett Laboratory, Imperial College, London SW7 2BZ, U.K.

J. T. Gosling, Los Alamos National Laboratory, Los Alamos, NM 87545.

R. G. Marsden and T. R. Sanderson, Space Science Department of European Space Agency, ESTEC, P.O. Box 299, 2200 AG Noordwijk, The Netherlands.

D. Lario, Applied Physics Laboratory, Johns Hopkins University, Laurel, MD 20723–6099. (david.lario@jhuapl.edu)

R. P. Lin, Space Sciences Laboratory, University of California, Berkeley, CA 94720.

M. Maksimovic, DESPA, Observatoire de Meudon, F-92195 Meudon, France.

S. P. Plunkett, USRA, Naval Research Laboratory, Washington, DC 20375.

B. Sanahuja, Departament d'Astronomia i Meteorologia, Universitat de Barcelona, Martí i Franquès 1, 08028 Barcelona, Spain. (e-mail: blai@am.ub.es)

(Received October 4, 1999; revised February 10, 2000;
accepted March 3, 2000.)